Nanoscale Horizons

ROYAL SOCIETY OF CHEMISTRY

MINIREVIEW

View Article Online
View Journal

Cite this: DOI: 10.1039/d5nh00676g

Emerging quantitative techniques for characterizing nucleic acid-involved molecular interactions

Ling Peng,[a] Yanxi Wang,[b] Mingguang Jin,[b] Ke Huang,*[a] Guan A. Wang*[b] and Feng Li*[bc]

Molecular interactions involving nucleic acids constitute a fundamental paradigm in biological systems, governing processes ranging from gene expression to cellular signaling. Quantitative characterization of the thermodynamic and kinetic parameters of these interactions is critical not only for deciphering molecular mechanisms but also for rational design in biomedical engineering and nanomaterials science. This review systematically surveys six major categories of quantitative methods used to study nucleic acid interactions: spectroscopic methods, separation-based methods, calorimetric methods, surface-based binding assays, single-molecule methods, and DNA nanotechnology-based methods. Each category is discussed with respect to its principal advantages and inherent limitations. While conventional methods such as electrophoretic mobility shift assays (EMSA), isothermal titration calorimetry (ITC), and spectroscopic titrations have provided foundational insights, they often exhibit constraints in sensitivity, throughput, or applicability under physiologically relevant conditions. Recent advances in DNA nanotechnology, leveraging its inherent programmability and structural precision, have enabled the development of novel quantitative platforms. These include DNA origami-based single-molecule methods and homogeneous assays that support accurate and native thermodynamic profiling, significantly enhancing sensitivity and adaptability in physiologically relevant contexts. This review systematically surveys established methodologies and critically evaluates emerging DNA nanotechnology-driven strategies, highlighting their potential to advance the quantitative analysis of nucleic acid interactions.

Received 2nd October 2025,
Accepted 5th December 2025

DOI: 10.1039/d5nh00676g

rsc.li/nanoscale-horizons

1. Introduction

Molecular interactions involving nucleic acids with other nucleic acids, proteins, or small molecules play a critical role across multiple research and application areas. Accurately measuring these interactions not only helps to reveal the regulatory mechanisms of essential biological processes like replication, transcription, and translation,[1–4] but also provides a fundamental basis for developing highly sensitive biosensors,[5–8] as well as novel drugs and molecular probes for clinical diagnosis and therapy.[8,9] For example, in the regulation of gene expression, proteins can recognize specific nucleic acid modifications, such as the m^7G cap structure, to maintain the translation of specific mRNAs under stress conditions, thereby helping to maintain cellular function.[2] During DNA replication, the dynamic binding between enzymes and nucleic acids directly influences the efficiency and accuracy of the process.[1] In the field of biosensing, the specific recognition between nucleic acid aptamers and viral proteins can be used to construct sensors with detection limits as low as the femtogram level, offering an efficient tool for the early diagnosis of infectious diseases.[5] Such methods combine high sensitivity with good adaptability, showing significant application potential. Furthermore, nucleic acid aptamers targeting viral proteins, such as DNA aptamers designed against the coronavirus nucleocapsid protein, can inhibit the replication of multiple variant strains with nanomolar affinity, suggesting a promising new approach for developing broad-spectrum antiviral drugs.[9] Therefore, establishing accurate, efficient, and universally applicable measurement methods is essential for advancing life science research and bioengineering applications.

This article provides a systematic review of techniques for the quantitative characterization of molecular interactions involving nucleic acids. Previous reviews have often focused on specific types of interactions, such as nucleic acid hybridization,[10]

[a] College of Chemistry and Material Science, Sichuan Normal University, Chengdu, Sichuan, 610068, China
[b] Key Laboratory of Green Chemistry and Technology of Ministry of Education, College of Chemistry, Sichuan University, Chengdu, Sichuan, 610064, P. R. China. E-mail: windtalker_1205@scu.edu.cn
[c] Med + X Center for Manufacturing, West China Hospital, Sichuan University, Chengdu, Sichuan, 610041, P. R. China

or the binding of nucleic acids with proteins[11] or small molecules,[12,13] and have summarized corresponding methodologies in detail. However, many of these approaches rely on specialized instruments and exhibit limited comparability across different methodological platforms.[14,15] They also typically require substantial sample amounts and specific experimental conditions, which may not accurately reflect the intracellular environment.[14] In recent years, certain single-molecule techniques, such as smFRET and optical tweezers,[16,17] have demonstrated advanced capabilities by enabling the direct manipulation and detection of individual nucleic acid molecules under applied forces.[18–20] Yet the consistency and standardization of their results still require further validation through additional reliable data and methodological improvements.

Notably, since the early 2000s, DNA nanotechnology-based methods have developed rapidly.[21] Leveraging the programmable nature, structural predictability, and ease of functionalization of nucleic acids, these methods have significantly improved detection flexibility and sensitivity.[22,23]

Unlike earlier reviews organized by the type of molecular target, this article categorizes existing methods based on their measurement principles into six groups: spectroscopic methods, separation-based methods, calorimetric methods, surface-based binding assays, single-molecule methods, and DNA nanotechnology-based methods (Fig. 1). Special emphasis is placed on DNA nanotechnology-based approaches, analyzing their design principles and application scenarios. By offering this principle-oriented perspective, this review aims to provide new insights and methodological references for both fundamental studies of nucleic acid interactions and the design of biosensors.

2. Conventional characterization methods

This section reviews established techniques for quantitatively characterizing interactions between nucleic acids and other molecules. These methods can be grouped into five categories based on their core principles: spectroscopic methods that rely on optical signal changes, separation methods that exploit differences in physical properties, thermal techniques that measure heat effects to determine thermodynamic parameters, surface-based binding assays that involve molecular immobilization, and single-molecule approaches that probe interactions at the individual molecule level. The following subsections will describe the basic principles and key parameters for each category, while also discussing their respective advantages and limitations. This overview aims to serve as a practical guide for selecting appropriate methods in different research contexts.

2.1. Spectroscopic methods

The binding of nucleic acids to ligands often induces measurable changes in optical signals, mass-to-charge ratios, or chemical shifts. Monitoring these changes allows researchers to determine key interaction parameters such as affinity, thermodynamics, and kinetics. Commonly used techniques include

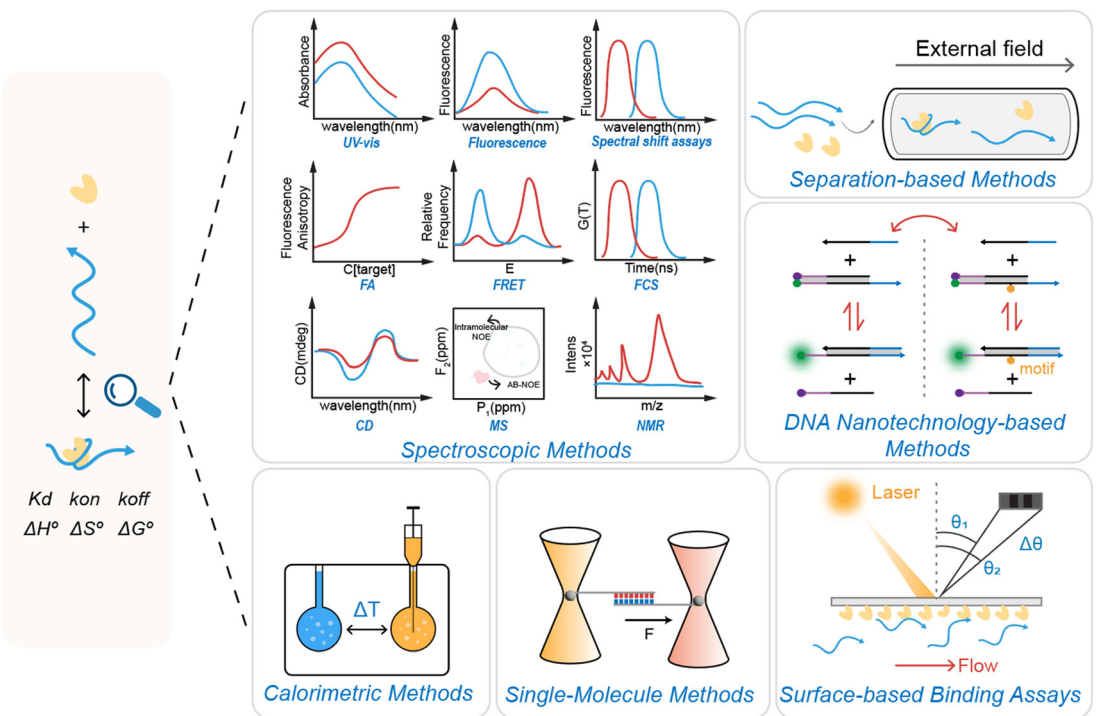

Fig. 1 Schematic overview of major methodologies for quantitative analysis of nucleic acid interactions, encompassing spectroscopic, separation-based, calorimetric, surface-based, single-molecule, and DNA nanotechnology-based methods.

UV-vis absorption spectroscopy,[24] fluorescence quenching, spectral shift assays (SpS),[25] fluorescence polarization/anisotropy (FP/FA),[26,27] Förster resonance energy transfer (FRET)/bioluminescence resonance energy transfer (BRET),[28,29] fluorescence correlation spectroscopy (FCS),[30] circular dichroism (CD),[31] mass spectrometry (MS),[32] and nuclear magnetic resonance (NMR).[33] Among these, methods based on changes in fluorescence intensity, such as FP/FA or FRET, remain popular choices due to their high sensitivity, relative simplicity, robustness, scalability, and cost-effectiveness. FP/FA has a long history of development. It measures changes in polarization resulting from the restricted rotation of fluorescently labeled nucleic acids upon binding to a target molecule, enabling direct determination of binding affinity in a homogeneous solution (Fig. 2a).[34] Usually, the smaller binding partner is fluorescently labeled as the fluorescent ligand, ensuring that changes in rotational diffusion upon complex formation can be sensitively detected.[26] Since its first application in studying DNA–protein interactions in the 1990s,[35] the technique has matured significantly. It is now widely used in aptamer research to quantify binding thermodynamics and kinetics for a broad range of targets in solution.[26] Its utility extends to other nucleic-acid recognition events as well. For instance, by using a FAM-labeled DNA-RNA hybrid chain, Zhang *et al.* observed an increase in fluorescence polarization upon binding of the S9.6 antibody,[36] reporting a dissociation constant (K_d) of 232 nM, which confirmed the high affinity and specificity of the antibody for the hybrid structure in R-loops.

FRET also serves as an essential tool for monitoring molecular interactions and dynamics at the nanoscale.[37] Its evolution has progressed from ensemble measurements to single-molecule detection,[16] and from equilibrium to kinetic studies.[38] Early bulk FRET experiments, based on titration, provided apparent K_d values at equilibrium but only reflected population averages. Time-resolved FRET (trFRET) can reduce background fluorescence interference and partially extract kinetic parameters, though its accuracy is limited by fitting methods. Single-molecule FRET (smFRET) represents a spectroscopic approach that enables single-molecule level resolution, allowing the characterization of molecular heterogeneity and conformational dynamics, although it requires highly sophisticated instrumentation and data analysis. Details are provided in Section 2.5. The subsequent development of kinetics FRET (kinFRET), which employs global fitting of single-molecule trajectories, allows for more accurate determination of association and dissociation rates, significantly enhancing kinetic studies.[38] Importantly, FRET is highly sensitive to conformational changes during binding,[39] providing dynamic structural information that is difficult to obtain with techniques like SPR.[19]

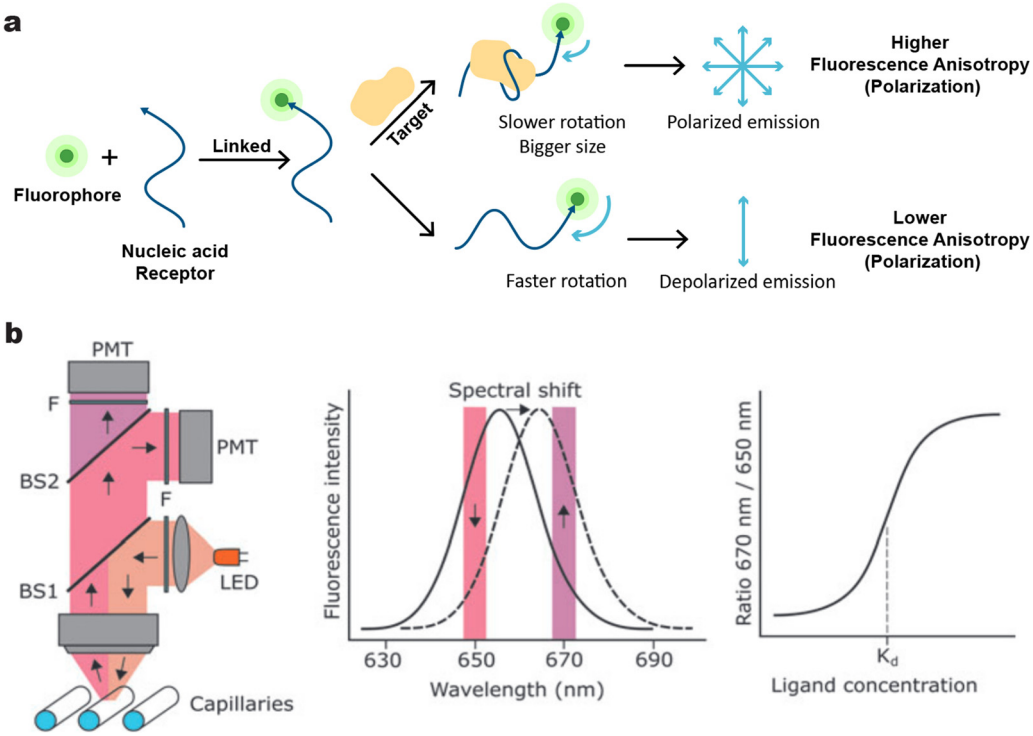

Fig. 2 Principles of fluorescence anisotropy and Spectral Shift (SpS) for quantitatively characterizing nucleic acid interactions. (a) Principle of nucleic acid–protein binding quantification by fluorescence anisotropy. Binding of a protein to a small, fluorescently labeled nucleic acid increases the molecular size and slows its rotational diffusion, thereby increasing the measured fluorescence anisotropy. (b) Schematic diagram of the quantitative characterization of interactions using SpS.[25] Upon ligand binding to a nucleic acid, a shift in the fluorescence emission wavelength occurs. The K_d can be determined with high sensitivity by monitoring the ratio ($R = F_{670}/F_{650}$) of fluorescence intensities at two wavelengths (*e.g.*, 650 nm and 670 nm). The linear relationship between K_d and temperature (T) can be used to derive the enthalpy change (ΔH) and entropy change (ΔS). Copyright 2022, Mary Ann Liebert, Inc.

Notably, the Spectral Shift (SpS) method, introduced in 2022,[25] is a novel strategy that utilizes environment-sensitive near-infrared dyes (*e.g.*, Cy5, Alexa647) labeled on the target molecule. A shift in the fluorescence spectrum is observed when ligand binding alters the dye's microenvironment (Fig. 2b). This method not only enables rapid ratiometric measurements at different temperatures with low sample consumption (only uses a few microliters of sample at low nanomolar concentration per data point) but can also be used to obtain thermodynamic parameters such as binding enthalpy and entropy, making it suitable for characterizing interactions between nucleic acid aptamers and dyes.[40] Studies have shown that a dye-to-base ratio between 0.7 and 3.0 is optimal; within this range, target binding induces a significant blue shift, and the magnitude of the shift correlates positively with binding strength for targets like ATP (detection limit 1.9 μM) or L-argininamide (detection limit 0.28 mM). Exceeding this ratio can disrupt the aptamer structure and reduce affinity, thus defining the practical operating window for SpS.[40]

Each method has its own advantages and limitations. Labeling-based approaches, such as FP/FA and FRET/BRET, provide high sensitivity but the labeling process may perturb the binding affinity of nucleic acids. Factors including the relative sizes of the ligand and target, fluorophore lifetime, and local rotational mobility can further influence measurement accuracy, requiring careful experimental design and optimization.[26] SpS enables rapid acquisition of thermodynamic data with low sample consumption and broad applicability, but its reliability depends on the sensitivity of the dye to local environmental changes. Many commercial dyes are optimized for environmental stability in other applications, such as FRET, which limits their suitability for SpS measurements.[25] It is also essential to ensure that dye labeling does not alter binding behavior. In contrast, label-free techniques such as CD spectroscopy, MS, and NMR provide complementary structural and compositional information. CD spectroscopy reveals nucleic acid conformational transitions,[41] but suffers from low spectral resolution, overlapping peaks,[42] and high sample concentration requirements.[43] MS can accurately determine molecular mass and complex stoichiometry,[32] whereas its gas-phase detection conditions restrict the quantification of binding affinities under physiological environments.[43] NMR enables atomic-level structural and kinetic characterization[33] but requires highly pure and concentrated samples.[44] Overall, these techniques collectively form a versatile toolkit for probing nucleic acid interactions, with each method involving inherent trade-offs between information depth, throughput, and experimental feasibility.

2.2. Separation-based methods

While spectroscopic methods monitor interactions within a solution, separation-based methods quantify binding events through the physical partitioning of bound and unbound species, offering a distinct approach to equilibrium analysis. Separation-based methods exploit differences in physical properties—such as charge, molecular size, or conformation—between bound and free molecules to achieve physical separation. Methods such as membrane dialysis, electrophoresis, thermophoresis, filtration, and chromatography enable the isolation of complexes,[26] and subsequent quantification of separated components allows the determination of affinity and binding stoichiometry (Fig. 3a). A key advantage of these approaches is the minimization of potential interference from other fluorescent species or nonspecific binding.

Specific methods include filter binding assays,[45] electrophoretic mobility shift assay (EMSA),[46] affinity capillary electrophoresis (ACE),[47] microscale thermophoresis (MST),[48] field-flow fractionation (FFF),[49] and liquid chromatography.[50] These techniques differ mainly in the driving force used for separation and the detection principle applied. Each has its own suitable scenarios in nucleic acid interaction studies. For instance, the electrophoretic mobility shift assay (EMSA) is widely employed as a classical method for the qualitative study of nucleic acid interactions, owing to its broad applicability (Fig. 3b).[46] However, EMSA is generally not suitable for investigating nucleic acid–small molecule interactions, since small molecules tend to diffuse through the gel during electrophoresis and contaminate the running buffer. Nevertheless, in certain well-designed systems where ligand binding induces pronounced conformational changes in the nucleic acid, such as specific aptamer–small molecule complexes, EMSA has been successfully applied to visualize binding-induced mobility shifts.[51] Although the technique can provide estimates of binding stoichiometry, affinity, and kinetic parameters under optimized conditions, its results remain semi-quantitative.[46,52] Furthermore, EMSA exhibits considerable variability in detection methodologies and involves complex experimental procedures that are prone to operational error. In contrast, ACE can measure binding affinities for various interactions, including those between nucleic acids and small molecules (Fig. 3c), offering high separation efficiency, short analysis time, and low sample consumption (nL range).[53] Importantly, ACE operates in an aqueous environment under near-physiological conditions.[47] By coupling capillary electrophoresis with fluorescence polarization detection, it is possible to accurately determine ligand affinity, characterize aptamer binding sites, develop multiplexed detection assays, and study binding stoichiometry in complex mixtures.[26] Recently, Huang's team successfully employed capillary electrophoresis-based systematic evolution of ligands by exponential enrichment (CE-SELEX) to isolate DNA aptamers with high affinity and specificity for the coronaviral nucleocapsid (*N*) protein.[9] The resulting six aptamers exhibited nanomolar affinity (1.31–135.36 nM) against N proteins from seven human-infecting coronaviruses and demonstrated significant antiviral activity.

Beyond equilibrium constants, ACE can also be used to obtain kinetic parameters. For example, Krylov's group developed kinetic capillary electrophoresis (KCE),[54] which analyzes the dissociation of complexes during electrophoresis to determine kinetic rate constants. In typical ACE assays, the target analyte concentration ranges from 0.1 nM to 100 μM, and the ligand concentration in the running buffer must exceed that of the injected analyte by at least one order of magnitude.[55]

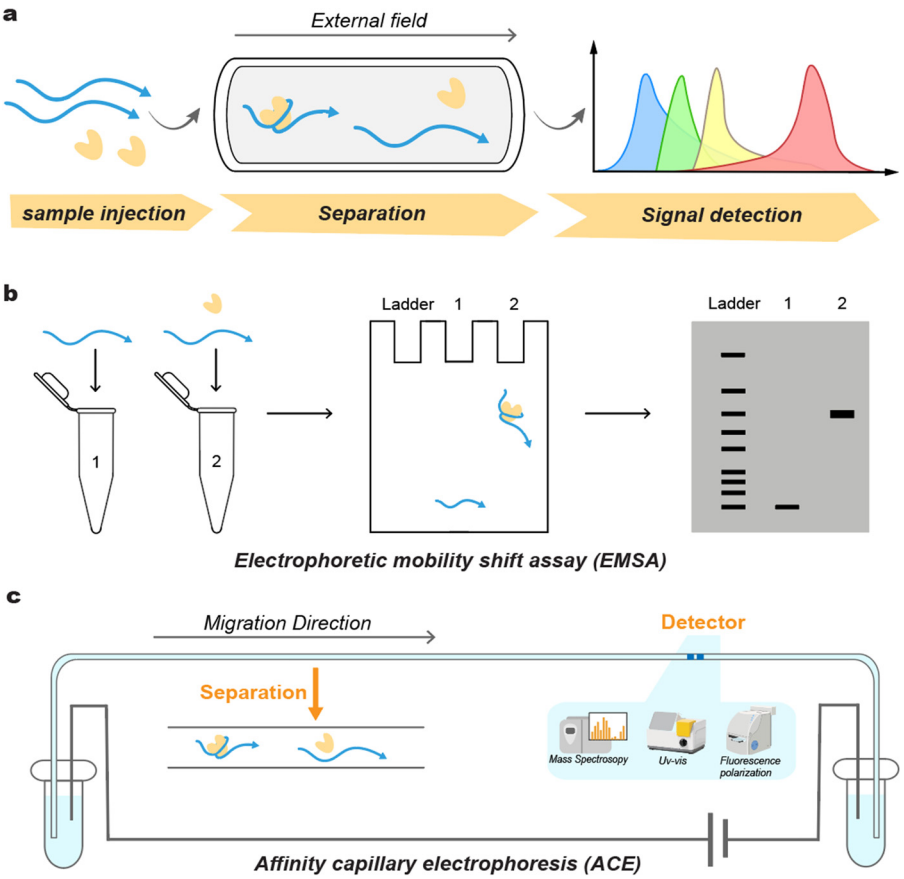

Fig. 3 Schematic diagrams of separation-based methods for studying nucleic acid-involved molecular interactions. (a) General principle of a separation assay, comprising three main steps: sample injection, separation under an external field (*e.g.*, electric), and signal detection. (b) Schematic illustration of the Affinity Capillary Electrophoresis (ACE) process. Under an applied electric field, nucleic acids and target molecules migrate directionally within the capillary. The formation of a complex reduces its migration rate compared to unbound molecules, enabling separation. The outlet end of the capillary is connected to a detection system, such as a mass spectrometer, UV-vis spectrophotometer, or microplate reader, for signal measurement. (c) Principle of the electrophoretic mobility shift assay (EMSA). A mixture of a nucleic acid probe and a protein is subjected to native gel electrophoresis. If binding occurs, the formed nucleoprotein complex has a larger size and lower mobility, resulting in a shifted band (lane 2) compared to the free probe (lane 1).

The total ligand solution volume required to fill the inlet and outlet vials, as well as the capillary, is approximately 1–2 mL.[56] This requirement can limit applications involving rare or low-abundance biomolecules, such as patient-derived disease-related oligonucleotides. To address this, Sueyoshi *et al.* introduced a partial filling technique under non-equilibrium conditions,[56] enabling high-throughput screening of interactions between small molecules and low-concentration oligonucleotides. This approach is suitable for strong-binding or fast-kinetics systems and allows simultaneous determination of the rates of association (k_{on}) and dissociation (k_{off}).

EMSA is commonly used for qualitative studies of nucleic acid interactions and offers broad applicability, though it typically provides only semi-quantitative information.[46] In contrast, ACE enables label-free analysis with high separation efficiency, low sample consumption, real-time monitoring of binding kinetics, and applicability to complex systems. However, ACE results can be influenced by buffer conditions, nonspecific adsorption, and electroosmotic flow.[47] MST is primarily employed to determine K_d but generally does not yield kinetic parameters, making it difficult to distinguish specific from nonspecific binding.[57] FFF, particularly when coupled with detectors such as multi-angle light scattering (MALS),[49] allows high-resolution separation under mild conditions across a broad size range (nanometers to hundreds of micrometers) and provides absolute parameters like molecular weight and binding stoichiometry. Nevertheless, FFF is limited by sample dilution, method complexity, and relatively low throughput. Liquid chromatography exhibits strong separation capability and compatibility with diverse detection systems; however, its requirement for microliter-level sample volumes and hundreds of milliliters of mobile phase results in significant consumption and higher operational costs.[55]

Beyond these analytical methods, binding affinities to native chromatin by sequencing (BANC seq) can also be conceptually categorized under separation-based approaches. Although it ultimately relies on next generation sequencing for readout, its core principle involves isolating and distinguishing bound from unbound DNA–protein complexes directly on native chromatin. The physical separation of chromatin fractions prior to

sequencing fulfills the same mechanistic criterion of resolving molecular populations based on binding state, thereby extending the separation-based framework into a genome wide context.[58,59]

2.3. Calorimetric methods

By measuring the intrinsic heat flux associated with binding, calorimetric methods actively probe interactions; this represents a key difference from spectroscopic and separation-based approaches, which monitor undisturbed equilibria. Calorimetric methods based on temperature changes monitor the heat effects (ΔH) associated with nucleic acid binding or conformational transitions, allowing direct determination of thermodynamic parameters. As these methods do not rely on fluorescence, radioactivity, or chemical labeling, they offer the advantages of being label-free, enabling *in situ* detection, and having low background interference. Commonly used methods include isothermal titration calorimetry (ITC) and differential scanning calorimetry (DSC).

ITC operates at constant temperature by incrementally titrating a ligand into the sample while recording the heat flow (μcal s^{-1}) in real time (Fig. 4a). By fitting the resulting data to a binding model, one can simultaneously obtain the K_d, ΔH, and stoichiometry (n), from which the free energy and entropy changes can be derived.[60] Recognized as the "gold standard" for thermodynamic characterization, ITC provides a complete set of binding parameters from a single experiment.[61] Recent advances also allow the derivation of kinetic parameters from calorimetric data.[62] ITC is applicable to a wide range of interactions involving nucleic acids with proteins or small molecules. To obtain accurate measurements, the nucleic acid like aptamer's concentration should generally exceed its K_d.[63] A common experimental setup uses ligand concentrations in the syringe that are 10–20 times higher than that in the cell, with typical conditions being 10–20 μM in the cell and 100–300 μM in the syringe.[60] This ensures near-saturation binding at 1 : 1 stoichiometry and complete complex formation

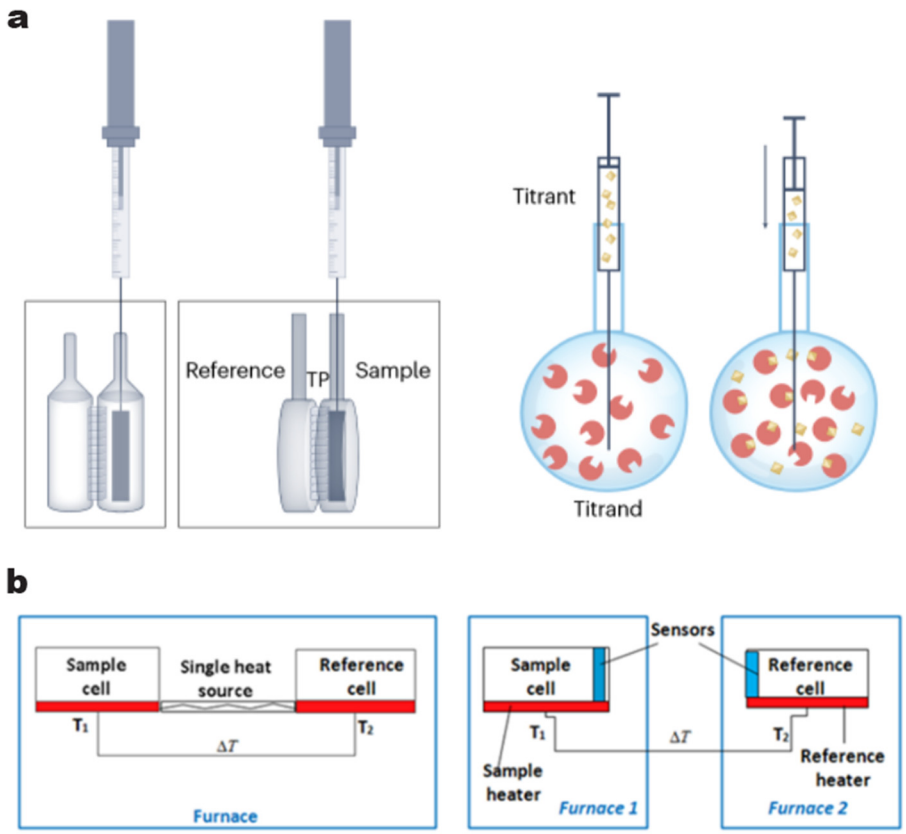

Fig. 4 Schematic diagrams of ITC and DSC instrumentation. (a) Schematic of an ITC instrument.[60] A cylindrical or coin-shaped sample cell and a reference cell are housed within an adiabatic jacket to ensure thermal isolation and maintain constant temperature. A stepper motor drives a gastight syringe to titrate ligand solution incrementally into the sample cell. A stirring device ensures rapid mixing after each injection. The temperature difference between the sample and reference cells is detected by a thermopile (TP) and converted into a voltage signal *via* the Seebeck effect, which is subsequently transformed into a heat power signal (left). When injected molecules (yellow squares) enter the reaction chamber, they bind to reactants (red circles with binding pockets) present in the solution, while unbound species remain free in solution (right). Copyright 2023, Springer. (b) Schematic of a DSC instrument.[66] In heat-flux DSC (left), both the sample and reference are placed in a single furnace. The temperature difference arising from thermal events in the sample is measured, and the instrument records the energy required to maintain isothermal conditions between the two, reflecting endothermic or exothermic processes. In power-compensation DSC (right), the sample and reference are housed in separate but identical furnaces. The instrument adjusts the power input to each furnace to maintain them at the same temperature, thereby directly measuring the thermal activity of the sample. Copyright 2016, MedCrave Group.

by the end of the titration.[64] Therefore, ITC is less suitable for weak binding systems with K_d values in the millimolar range, as the high nucleic acid concentrations required result in significant sample consumption and cost, and may promote intermolecular association of DNA at such elevated concentrations.[43] In contrast, for high-affinity binders at the nanomolar level or stronger, a displacement titration strategy can be employed to extend the usable range of ITC, enabling full thermodynamic characterization of picomolar-affinity ligands.[64] Nevertheless, ITC remains limited by instrumental expense and substantial sample requirements.[60] Consequently, it is often used in combination with other techniques. For example, Zhang's team used ITC to determine a K_d of 1–4 μM and a N of approximately 0.8 for the interaction between an SPT6 construct and the U1A protein within the Pol II-DSIF-SPT6-U1 snRNP transcription elongation complex.[65] These results not only validated the binding interface observed by cryo-electron microscopy but also revealed a direct interaction between the transcription factor and the splicing factor.

DSC, in contrast, measures heat absorption changes during programmed heating, which occur during folding/unfolding or complex dissociation (Fig. 4b).[67] It accurately determines the melting temperature (T_m) and ΔH, making it suitable for studying weak interactions (in the high μM to mM range) that are challenging for other techniques like ITC.[13] This technique is particularly valuable for assessing the effects of environmental conditions or chemical modifications on nucleic acid thermal stability and can simultaneously resolve the thermodynamics of folding processes and binding reactions. Therefore, DSC holds significant application value in drug discovery and the study of complex biomolecular interactions.[68]

In summary, ITC enables direct measurement of the heat effects associated with binding reactions under constant temperature conditions, providing a complete set of thermodynamic parameters from a single experiment. This approach offers model-independent and quantitatively precise results. However, ITC requires substantial sample quantities, has low throughput, and is less suitable for characterizing weak interactions. Similarly, DSC allows direct acquisition of experimental thermal data without assuming a binding mechanism, permitting high-precision characterization of thermodynamic processes. DSC is highly sensitive to temperature-induced conformational transitions and can be used to detect nucleic acid duplex melting, oligonucleotide secondary structure changes, and stability variations caused by ligand binding. Nevertheless, DSC also suffers from low throughput, provides only global thermal responses under equilibrium conditions, and is unable to resolve local or transient structural changes. Furthermore, its strict requirements for buffer compatibility and the complexity of thermal drift correction limit its application in complex biological systems.[66]

2.4. Surface-based binding assays

A critical requirement for many studies is the acquisition of real-time kinetic data, which is uniquely addressed by surface-based binding assays. In these approaches, nucleic acids are immobilized on a solid support and their interaction with ligands in a flowing solution is monitored, enabling label-free analysis and detailed kinetic profiling. Representative techniques include surface plasmon resonance (SPR), bio-layer interferometry (BLI), and quartz crystal microbalance (QCM), each with distinct detection principles and application scopes.

SPR has been used for affinity measurement for over 30 years[69] and was applied to study various molecular interactions involving nucleic acids around the year 2000.[70] SPR detects molecular binding events by monitoring changes in the refractive index near a thin metal film coating a glass substrate (Fig. 5a).[71] When a nucleic acid in the solution binds to an immobilized ligand on the sensor chip, it causes a shift in the resonance angle, which is observed as a change in reflected light intensity. This provides real-time binding and dissociation curves, from which the k_{on}, k_{off} and K_d can be derived.[72] For instance, Miggiano *et al.* used SPR to study the binding of *Mycobacterium tuberculosis* UvrA protein and its mutants to damaged DNA. They found that while a mutant could still bind, its significantly faster k_{off} and reduced response prevented the complex from reaching a stable state, explaining why it was missed by traditional, non-real-time methods like EMSA and MST.[73] SPR is considered a gold standard for studying interactions in flow due to its high sensitivity, low sample consumption, and ability to detect weak binding and small molecules. However, optimization of the immobilization strategy is required to minimize non-specific adsorption caused by the negative charge of nucleic acids.[72,74]

BLI, alongside SPR, is one of the most commonly used techniques for studying biomolecular interactions and kinetics. BLI measures changes in the thickness of a biological layer on the tip of a fiber-optic biosensor in real time, which manifests as a shift in the interference spectrum wavelength (Fig. 5b). This allows direct determination of kinetic parameters during association and dissociation phases.[57] BLI offers several practical advantages over SPR. It eliminates the need for a microfluidic system, simplifies maintenance, and provides higher throughput. Its enhanced compatibility with diverse buffer components and small molecules further makes it ideal for high-throughput screening. These characteristics make BLI particularly suitable for high-throughput screening. In nucleic acid research, BLI is widely used for aptamer screening, drug discovery, and target validation. To illustrate this utility in aptamer development, Zhang *et al.* used BLI integrated with the high-throughput platform FAIVE (Functional Aptamers *in vitro* Evolution) to rapidly evaluate the affinity of candidate anti-HIV-1 aptamers, identifying a TAR RNA-binding aptamer with a K_d of approximately 9 nM, an over 10-fold improvement compared to previously reported aptamers. The FAIVE platform itself represents an innovative *in vitro* selection method that integrates affinity selection with functional screening in a single workflow. It introduces chemical diversity through click-chemistry-modified nucleotide libraries and employs fluorescence-activated cell sorting (FACS) to directly and rapidly screen large particle libraries, thereby enriching aptamers that not only bind strongly but also regulate target function.[76]

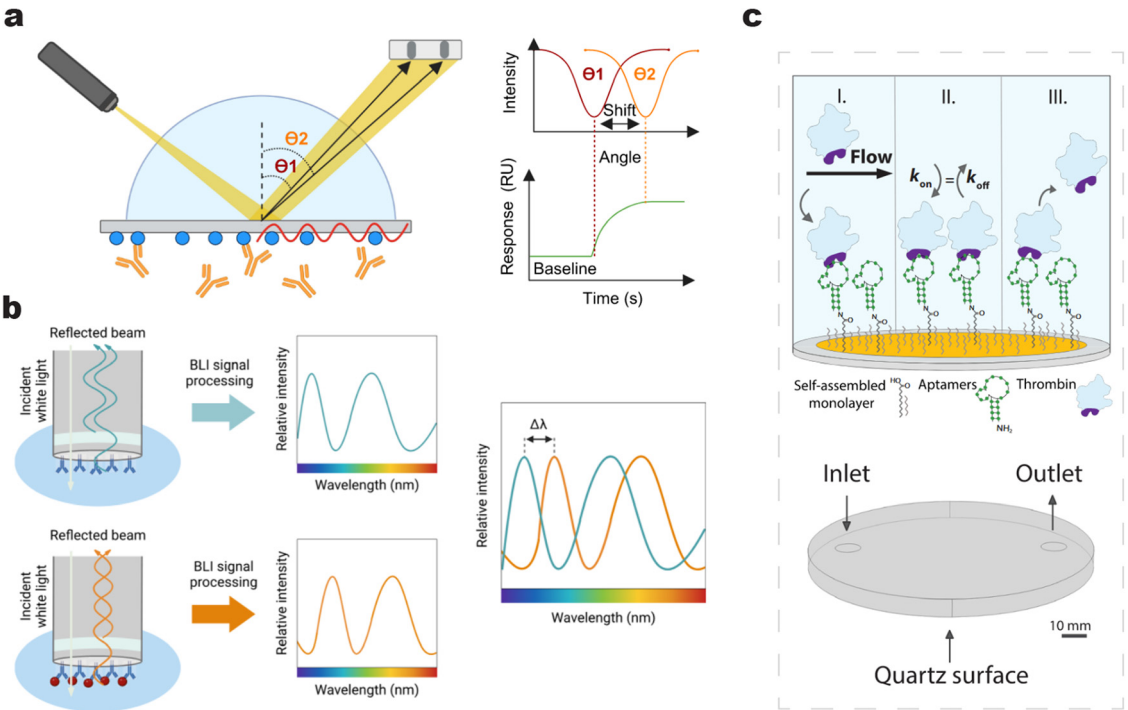

Fig. 5 Principles of surface-based techniques for quantitative characterization of nucleic acid interactions. (a) Surface plasmon resonance (SPR).[75] A beam of polarized light is directed toward a metal-coated sensor surface. The shift in the resonance angle from θ_1 to θ_2, caused by changes in refractive index upon molecular binding, is detected in real time. Copyright 2024, Dove Medical Press Limited. (b) Bio-layer interferometry (BLI).[57] White light is incident on the biosensor tip, and reflected light interferes to generate an interference spectrum. Binding-induced changes in optical thickness result in a wavelength shift ($\Delta\lambda$), which is monitored over time. Copyright 2024, Elsevier. (c) Quartz crystal microbalance (QCM).[19] The sensor surface is functionalized with an aptamer monolayer. Upon binding of the target protein, the change in mass deposited on the quartz crystal leads to a decrease in its resonance frequency (Δf). Copyright 2025, The American Association for the Advancement of Science.

In another application showcasing its screening capabilities, Sandra *et al.* efficiently screened a microbial metabolite library using BLI and identified three natural products with high DNA-binding activity, demonstrating the technique's potential in natural product discovery and functional molecule screening.[77]

QCM relies on the high sensitivity of a piezoelectric quartz crystal's resonance frequency to mass changes on its surface.[78] It monitors binding events in real time and can simultaneously reflect changes in mass and viscoelastic properties, making it especially useful for studying conformational rearrangements or surface adsorption behavior accompanying nucleic acid binding (Fig. 5c). In the development of a thrombin biosensor, Joo *et al.* used QCM to monitor the frequency shift (Δf) caused by aptamer–protein binding.[19] They quantitatively showed that the rate constants were better predictors of sensor performance (such as sensitivity and detection limit) than the affinity constant alone. Using structurally similar aptamers as models, QCM validated single-molecule kinetic decoding results: although the three aptamers had similar K_d values, the combination of a fast k_{on} and a slow k_{off} significantly improved detection efficiency, providing a kinetic basis for the rational design of highly responsive nucleic acid sensors.

Despite their advantages, these surface-based methods have limitations. Firstly, immobilization onto a solid phase can potentially alter the conformation or reduce the activity of the biomolecules. When a nucleic acid or ligand is fixed to the sensor surface, its spatial conformation and freedom of movement may be restricted, leading to binding behavior that differs from that in free solution. Secondly, non-specific adsorption and background interference can be significant. The inherent negative charge of nucleic acids makes them prone to electrostatic or hydrophobic interactions with the sensor surface or probe molecules, which can compromise the accuracy and reliability of quantitative results.

In summary, SPR enables label-free, real-time detection with high sensitivity, reusable sensor chips, and simultaneous acquisition of kinetic and thermodynamic parameters. However, the technique requires relatively high instrumentation costs and involves complex operational procedures.[74] BLI eliminates the need for microfluidic systems, simplifies maintenance, and is suitable for analyzing low-molecular-weight analytes (down to 150 Da) as well as high-throughput screening. Nevertheless, this method may compromise some degree of data accuracy and reproducibility.[57,79] QCM offers a simple instrumental setup, label-free operation, sub-nanometer-level sensitivity, affordability, and broad adaptability. A limitation, however, is that its measurements can be influenced by interfacial parameters such as surface roughness, free energy, and charge distribution.[78]

2.5. Single-molecule methods

The methods covered thus far primarily report on ensemble-averaged properties. Single-molecule techniques, however,

overcome this limitation by resolving discrete states and transient intermediates within a heterogeneous population, thereby offering unique insights into kinetic pathways and molecular heterogeneity. Single-molecule methods enable the direct manipulation and detection of individual nucleic acid molecules under applied forces, allowing thermodynamic and kinetic characterization of interactions at the molecular level.[20] Common methods include optical tweezers (OT),[17] magnetic tweezers (MT),[80] atomic force microscopy (AFM),[81] single-molecule FRET (smFRET),[82] tethered particle motion (TPM),[83] and DNA flow-stretching assays.[18]

OT use a highly focused laser beam to exert piconewton-scale forces on a dielectric bead attached to a nucleic acid, permitting real-time observation of conformational changes, binding, and dissociation events (Fig. 6a).[17] smFRET measures the efficiency of energy transfer between donor and acceptor fluorophores, which is sensitive to distances in the 3–8 nm range, providing access to association/dissociation rates, conformational lifetimes, and free energy differences.[16] However, its utility can be limited by photophysical artifacts of the dyes, the short distance range, and potential alterations of molecular activity due to labeling. MT manipulate the end of a nucleic acid molecule attached to a magnetic bead, applying controlled forces and torques to measure critical unzipping forces, supercoiling density, and torsional energy storage (Fig. 6b).[84] Their spatial resolution is generally lower (approximately 5–10 nm), making it challenging to capture very brief transient states. AFM uses a nanoscale tip to scan and manipulate single molecules, providing sub-nanometer spatial resolution of features such as complex height, and allowing quantification of unfolding energies and adhesion forces (Fig. 6c).[85] A limitation is its susceptibility to surface interactions, and it is less suited for tracking rapid dynamics. For example, Joo *et al.* developed a technique on an smFRET platform to decode aptamer–protein interactions, using thrombin as the analyte and the structurally similar aptamers HD1, RE31, and NU172 as biorecognition elements.[19] This approach robustly quantified k_{on}, k_{off}, and K_d. While the aptamers had similar dissociation constants,

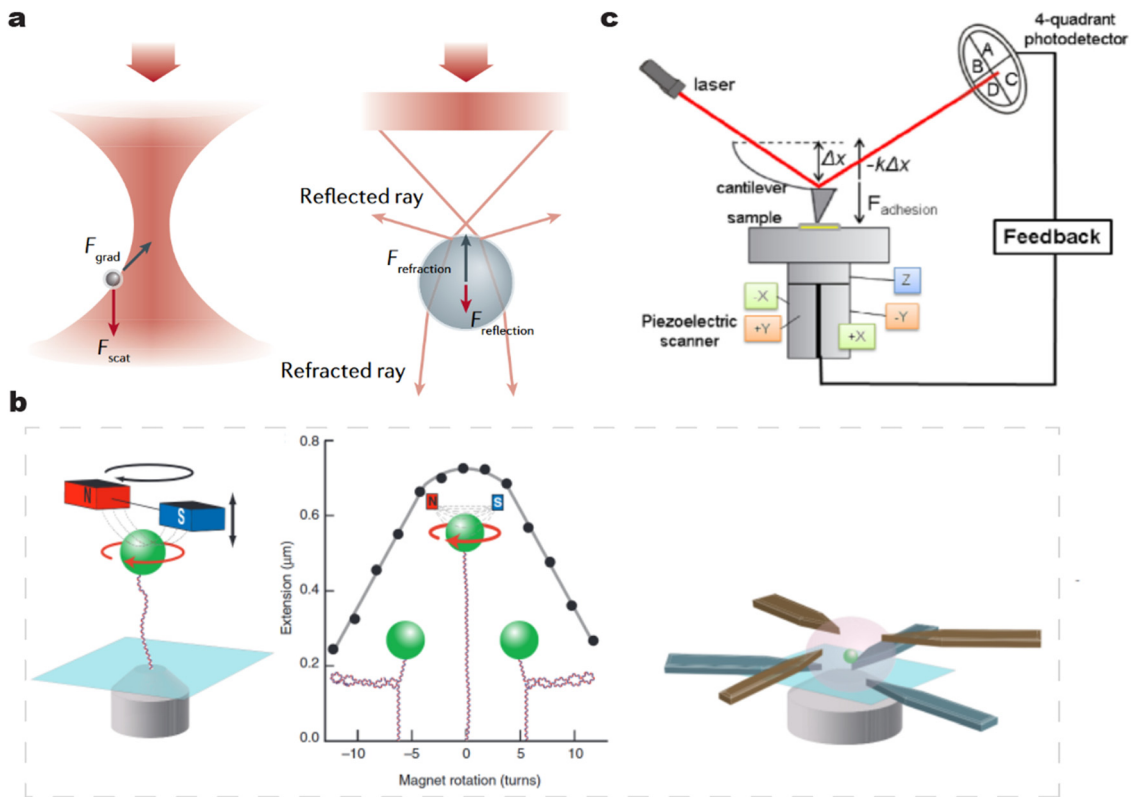

Fig. 6 Principles of single-molecule methods for quantitative characterization of nucleic acid interactions. (a) Optical tweezers (OT).[17] A highly focused laser beam forms an optical trap to capture a dielectric bead attached to a nucleic acid molecule. The gradient force (F_{grad}) pulls the bead toward the focal point, while the scattering force (F_{scat}) acts along the light propagation direction. By monitoring bead displacement *via* back-focal-plane interferometry, piconewton-scale forces and nanometer-scale displacements can be measured in real time. Copyright 2021, Springer. (b) Magnetic tweezers (MT).[86] A nucleic acid molecule is tethered between a surface and a superparamagnetic bead. Electromagnets (N–S poles) generate controlled magnetic fields to apply precise forces or torques to the bead. The bead's vertical position (extension) is tracked under varying magnet rotations, allowing measurement of DNA twist, supercoiling, and protein-induced conformational changes. The plot shows a characteristic extension–rotation curve with distinct states (R, S), reflecting torsional responses to mechanical manipulation. Copyright 2008, Springer. (c) Atomic force microscopy (AFM).[81] A sharp cantilever with a functionalized tip scans the sample surface. A laser beam reflects off the cantilever onto a four-quadrant photodetector (A, B, C, D segments). Tip–sample interactions like adhesion forces ($F_{adhesion}$) cause cantilever deflection (Δx), detected as differential photocurrents. A piezoelectric scanner (*X*, *Y*, *Z* axes) controls tip position with sub-nanometer precision, while a feedback loop maintains constant force during imaging or force spectroscopy. Copyright 2023, Elsevier.

their association and dissociation rate constants differed substantially, highlighting distinct underlying binding mechanisms. These findings were validated with computational simulations and QCM experiments, demonstrating how the method can aid the rational selection of aptamers with tailored binding properties.

Overall, these single-molecule techniques offer unique capabilities for probing biomolecular interactions. However, they are also accompanied by distinct technical limitations. For instance, OT are limited by low throughput and susceptibility to photodamage and thermal effects.[17] In contrast, MT provide gentle manipulation and can operate in complex biological environments, making them well-suited for low-force (subpiconewton) studies. Nevertheless, MT exhibit limited spatial resolution (approximately 5–10 nm), making it difficult to capture rapid transient conformational changes, and offer relatively limited manipulation dimensionality.[86] Similarly, smFRET monitors distance changes within the 3–8 nm range, providing direct access to binding kinetics and thermodynamic parameters. However, its application can be constrained by photobleaching, fluorophore artifacts, and potential perturbations introduced by labeling. AFM covers the broadest force detection range (10–10^4 pN), allows experiments under near-physiological liquid conditions, and can be combined with imaging for nanoscale resolution. It yields mechanical strength, activation free energy, zero-force dissociation rate constants, transition state distance, and complex lifetime data without requiring fluorescent labels or metal coatings.[81] A key limitation is its lower force resolution due to the large size and high stiffness of the probes, alongside susceptibility to non-specific adsorption.[86] Furthermore, techniques like TPM and flow-stretching assays provide higher throughput and operational simplicity for monitoring conformational fluctuations over long timescales at low forces, serving as effective complementary approaches. This diverse toolkit enables a fundamental advantage over traditional ensemble methods: the direct measurement of binding forces, lifetime distributions, and intermediate states at the level of individual molecules. This reveals microscopic heterogeneity that is often hidden in bulk measurements, offering unparalleled resolution and sensitivity. Notwithstanding these powerful advantages, a primary limitation common to all these single-molecule methods is the high level of expertise required for experimental design and data analysis, which remains a significant barrier to their more widespread application.

In summary, while conventional techniques such as spectroscopic, separation-based, calorimetric, surface-binding, and single-molecule methods have provided valuable tools for quantifying nucleic acid interactions, they also come with certain constraints. These include reliance on specialized instrumentation, variations in data comparability across platforms, and limitations in capturing weak interactions or complex biological contexts. Such considerations point to the value of developing complementary approaches that may offer greater flexibility and better reflect physiological conditions. In this context, DNA nanotechnology has emerged as a promising direction. As will be discussed in the following section, methods based on DNA nanotechnology seek to provide another approach to achieve high-quality data that can enhance our understanding of nucleic acid interactions beyond the scope of traditional techniques.

3. DNA nanotechnology-based methods

The preceding section has outlined conventional methods for studying nucleic acid interactions. These approaches generally exhibit limited comparability across different platforms and require further validation through additional reliable data and methodological improvements. Therefore, there is a clear need to develop molecular tools capable of accurately characterizing the relevant thermodynamic and kinetic parameters. Recently, DNA-based approaches have been developed that exploit a simple principle: thermodynamic properties can be derived from equilibrium shifts in DNA-mediated reactions. For a specific nucleic acid motif, such as its folding energy, the thermodynamic parameters are determined by comparing its equilibrium state with reference probes of known parameters within the same reversible reaction system. The main advantage of these DNA-based methods lies in their ability to analyze the thermodynamics of nucleic acid structures or modifications under native conditions.

3.1. Introduction to dynamic DNA nanotechnology

The development of DNA-based molecular tools builds upon the foundation of dynamic DNA nanotechnology. This field has evolved from creating static structures to engineering systems capable of programmable motion, reconfiguration, and computation at the nanoscale.[87] By harnessing the predictable base pairing of DNA, researchers design nanostructures that respond to specific molecular inputs or environmental changes, enabling diverse applications in biosensing, drug delivery, and molecular machinery.[88–93] A fundamental mechanism enabling this transition is DNA strand displacement, where an incoming DNA strand binds to a short single-stranded toehold region and replaces a pre-hybridized strand.[87] This process allows precise control over reaction kinetics and facilitates complex functions including catalytic amplification, logic operations, and autonomous motion.[94–97]

DNA's programmability stems from its well-characterized thermodynamics and kinetics, which support the design of highly specific structures. Early research in DNA nanotechnology primarily focused on static assemblies such as geometric shapes constructed using double-crossover tiles.[98] The incorporation of dynamic elements, particularly toehold-mediated strand displacement, has expanded possibilities to include reconfigurable systems. For instance, DNA tweezers can repeatedly transition between open and closed states through sequential addition of fuel strands,[99] demonstrating how nucleic acids can serve as nanoscale actuators. Reaction kinetics can be systematically tuned by adjusting toehold length and

sequence, providing a versatile platform for engineering responsive molecular devices. Comprehensive reviews covering these fundamental concepts and their applications are available for further reference.[87,95–97]

Among various toehold activation strategies, the toehold-exchange mechanism stands out as one of the most powerful and widely used designs. Its key characteristic is reversibility, which is regulated by forward and reverse toeholds. By adjusting toehold length, sequence, or reactant stoichiometry, the reaction free energy can be precisely tuned to approach zero, resulting in an equilibrium yield of approximately 50%. Small thermodynamic perturbations can then shift this equilibrium and produce significant changes in yield. Furthermore, the forward and reverse reaction kinetics remain effectively decoupled, enabling a rapid system response. Due to this high sensitivity toward thermodynamic changes, toehold-exchange systems have been extensively applied for detecting single nucleotide variants (SNVs) against wild-type sequences.[91,100–104] In principle, determining thermodynamic parameters for nucleic acids shares similarities with distinguishing SNVs from wild-type sequences. In summary, dynamic nucleic acid circuits based on intermolecular reversible reactions provide a robust platform for detecting thermodynamic differences caused by structural or chemical modifications. The following section will illustrate applications of DNA nanotechnology-based methods in studying molecular interactions.

3.2. DNA reaction-based molecular tools

The research group led by David Yu Zhang developed and experimentally verified a DNA reaction-network method for directly measuring the thermodynamic properties of nucleic acid structural motifs. In their initial study, they used a non-covalent catalytic circuit to systematically determine the free energies of all base-dangling ends.[22] This approach builds on the nearest-neighbor model, where the total free energy equals the sum of individual non-overlapping structural components (Fig. 7a). In contrast to melting-based methods that depend on extrapolation to estimate thermodynamic parameters,[105,106] this technique allows direct determination of free energy values under native, isothermal conditions of interest, while still relying on the fundamental thermodynamic principles established by melting-based approaches.

The net equilibrium reaction is driven by dangle stacking, wherein strand X displaces pre-hybridized Y and forms a dangle terminus (Fig. 7b). Due to the absence of a toehold domain, the kinetics are too slow for practical application. To address this, a catalyst strand C is introduced. It first reacts with the YZ duplex to generate an active intermediate CZ, enabling strand X to rapidly form the product duplex XZ (Fig. 7c). The free energy of the net displacement reaction can be calculated as:

$$\begin{aligned}\Delta G^{\circ}_{\mathrm{rxn}} &= \Delta G^{\circ}_{\mathrm{XZ}} + \Delta G^{\circ}_{\mathrm{Y}} - \Delta G^{\circ}_{\mathrm{X}} - \Delta G^{\circ}_{\mathrm{YZ}} \\ &= \left(\Delta G^{\circ}_{\mathrm{XZ}} - \Delta G^{\circ}_{\mathrm{YZ}}\right) + \left(\Delta G^{\circ}_{\mathrm{Y}} - \Delta G^{\circ}_{\mathrm{Z}}\right)\end{aligned} \quad (1)$$

where the term $\left(\Delta G^{\circ}_{\mathrm{XZ}} - \Delta G^{\circ}_{\mathrm{YZ}}\right)$ equals the dangle-stacking motif $\Delta G^{\circ}_{\mathrm{motif}}$, and $\left(\Delta G^{\circ}_{\mathrm{Y}} - \Delta G^{\circ}_{\mathrm{Z}}\right)$ approximates zero when

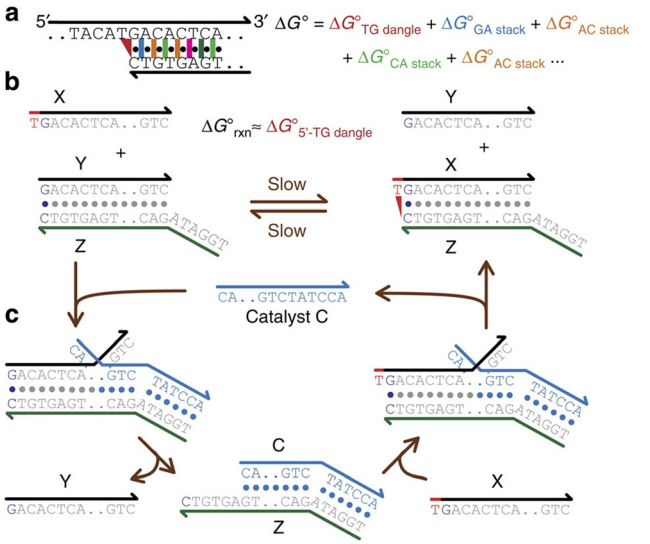

Fig. 7 Schematic illustration of a DNA circuit for measurement of the free energy of the dangling end.[22] (a) The overall free energy of nucleic acid hybridization is a summation of all non-overlapping DNA motifs. (b) The net reaction of strand displacement, which is kinetically accelerated by a catalytic circuit. (c) A non-covalent catalytic circuit designed to kinetically accelerate the strand displacement reaction toward equilibrium. Copyright 2016, Springer.

sequences are appropriately designed to avoid secondary structures. The value of $\Delta G^{\circ}_{\mathrm{rxn}}$ can be experimentally determined from equilibrium concentration observations. Collectively, the dangle stacking free energy is measured according to eqn (2).

$$\Delta G^{\circ}_{\mathrm{rxn}} = -RT\ln\left(K_{\mathrm{eq}}\right) = -RT\ln\left(\frac{[\mathrm{Y}]_{\mathrm{eq}}\cdot[\mathrm{XZ}]_{\mathrm{eq}}}{[\mathrm{X}]_{\mathrm{eq}}\cdot[\mathrm{YZ}]_{\mathrm{eq}}}\right) = \Delta G^{\circ}_{\mathrm{motif}} \quad (2)$$

where R and T stand for the gas constant and temperature in Kelvin, respectively.

To ensure the validity of this reaction model, it is essential to maintain low concentrations of intermediate species. Short-lived complexes such as CXZ and CYZ can be neglected in the analysis. However, since the CZ duplex has free energy comparable to the YZ and XZ duplexes, it can accumulate during the catalytic cycle. To minimize potential errors, the catalyst concentration C is kept sufficiently low, limiting possible overestimation to within 0.2 kcal mol^{-1}.

Using this non-covalent catalytic approach, Zhang's team determined the standard free energy contributions (ΔG°) of various modifications, including fluorophores and single- or multi-nucleotide dangling ends. Interestingly, the results revealed contrasting effects: while the first dangling nucleotide stabilized the structure, additional nucleotides caused destabilization due to electrostatic repulsion. These findings establish dangling end length as an important factor for refining standard models of DNA hybridization and folding. Overall, this direct measurement approach demonstrated better accuracy than methods relying on extrapolation through linear algebra decomposition.

Expanding their catalytic circuit methodology, Zhang and colleagues created the toehold exchange energy measurement (TEEM) platform for direct thermodynamic characterization of nucleic acid interactions (Fig. 8a).[107] By labeling the CP reporter duplex with a fluorophore-quencher pair, they could quantitatively monitor reaction yields (Fig. 8b). Here, CP and CX helices served as negative and positive controls, respectively. Once the TEEM reaction yield was determined, the corresponding free energy values were calculated (Fig. 8c):

$$\Delta G^{\circ}_{\mathrm{rxn}} = -RT\ln\left(K_{\mathrm{eq}}\right) = -RT\ln\left(\frac{y\cdot\left([\mathrm{P}]_0 + y\right)}{\left([\mathrm{CP}]_0 - y\right)\cdot\left([\mathrm{X}]_0 - y\right)}\right) \tag{3}$$

where y is the concentration of CX formed.

To validate the robustness of their approach, the researchers measured reaction free energies across a temperature range from 25 °C to 67 °C (Fig. 8d). The free energy *versus* temperature profile showed a curved pattern, indicating that the enthalpy change (ΔH°) and entropy change (ΔS°) of the toehold-exchange reaction varied with temperature—had they remained constant, the relationship would have been linear according to eqn (2). For structural motifs such as bulges, free energy values were obtained by subtracting the ΔG° of the motif-containing reaction from that of a reference system (Fig. 8e). To ensure accuracy, the strands X_{ref} and X_{motif} were designed to avoid significant secondary structure formation. Using a cTa bulge as a model, the measured free energy remained nearly constant over a wide temperature range (Fig. 8f), consistent with high-resolution melting (HRM) data collected near the melting temperature where HRM is most accurate.

$$\begin{aligned}
&\Delta G^{\circ}_{\mathrm{rxn,motif}} - \Delta G^{\circ}_{\mathrm{rxn,ref}} \\
&= \left(\Delta G^{\circ}_{\mathrm{CX,motif}} + \Delta G^{\circ}_{\mathrm{P}} - \Delta G^{\circ}_{\mathrm{CP}} - \Delta G^{\circ}_{\mathrm{X,motif}}\right) \\
&\quad - \left(\Delta G^{\circ}_{\mathrm{CX,ref}} + \Delta G^{\circ}_{\mathrm{P}} - \Delta G^{\circ}_{\mathrm{CP}} - \Delta G^{\circ}_{\mathrm{X,ref}}\right) \\
&\approx \Delta G^{\circ}_{\mathrm{CX,ref}} - \Delta G^{\circ}_{\mathrm{CX,ref}} \\
&= \Delta\Delta G^{\circ}_{\mathrm{motif}}
\end{aligned} \tag{4}$$

As noted, positioning the reaction yield near 50% minimizes errors in free energy estimation for a given yield variation. However, simultaneously optimizing both motif and reference reactions is challenging. Larger values of $\Delta\Delta G^{\circ}_{\mathrm{motif}}$ increase measurement error, limiting accurate quantification to approximately 4 kcal mol^{-1}.

Concurrently, Li's group recognized the potential of toehold exchange as a measurement platform and introduced the DNA balance method.[108] The core reaction resembled TEEM but employed a set of invader strands with systematically varied toehold designs, termed Weight strands, to drive the reaction (Fig. 9a). This panel generated a range of reaction yields corresponding to different $\Delta G^{\circ}_{\mathrm{rxn}}$ values. The same weight panel was applied to both reference and motif-containing reporters, and the free energy was determined by comparing the Yield-$\Delta G^{\circ}_{\mathrm{rxn}}$ standard curves (Fig. 9b). The process for the reference reporter was described as "taring", similar to zeroing a balance, while that for the motif reporter was termed "weighing".

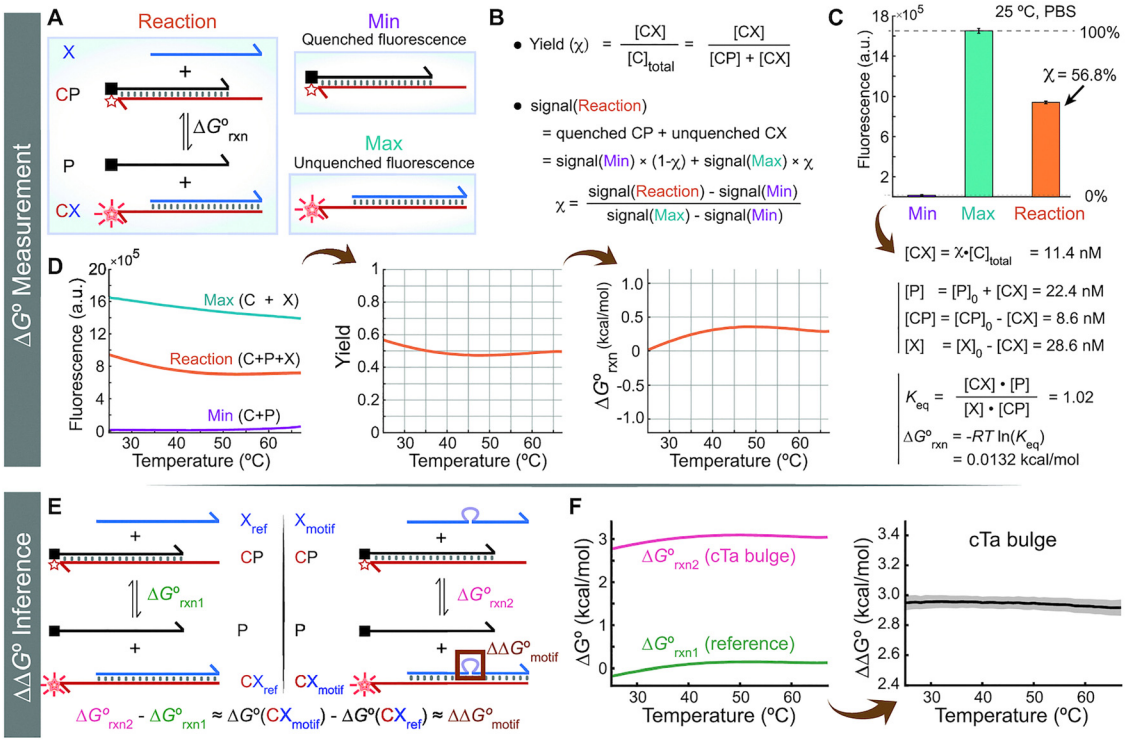

Fig. 8 The mechanism of TEEM and calculation process of free energy values from observed reaction yields.[107] Copyright 2020, Oxford University Press.

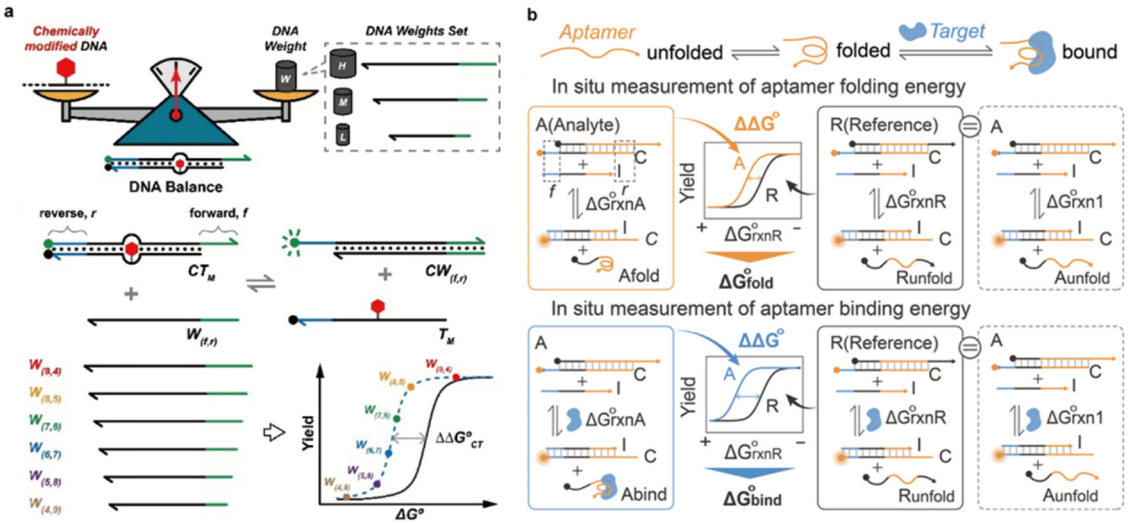

Fig. 9 (a) Schematic representation of the concept of DNA balance with a library of weigh strands.[108] (b) Schematic representation of the concept of free energy shift assay (FESA) for characterizing the folding thermodynamics of noncanonical nucleic acid structures.[109] Copyright 2021, American Chemical Society.

This strategy eliminates the need to fine-tune the yield to 50% and does not require prior estimation of free energies. To demonstrate utility, the authors measured thermodynamic parameters of a thermally responsive cyclic azobenzene modification, which conventional melting-based methods cannot accurately characterize. Using the DNA balance, these parameters were determined for the first time under native conditions.

In the methods described above, measurements rely on direct quantification of $\Delta\Delta G^{\circ}_{\mathrm{rxn}}$ between analyte and reference reactions. This works well for simple motifs like bulges but not for complex systems such as non-canonical structure folding, where folding energy does not have a simple linear relationship with observed yield. To address this limitation, Wu *et al.* developed the free energy shift assay (FESA), which enables characterization using eqn (5) and (6):[109]

$$e^{-\frac{\Delta\Delta G_{\mathrm{balance}}}{RT}} = e^{-\frac{\Delta G^{\circ}_{\mathrm{fold}}}{RT}} + 1 \quad (5)$$

$$e^{-\frac{\Delta\Delta G_{\mathrm{balance}}}{RT}} \approx \frac{[\mathrm{Ligand}]_0}{K^{\circ}_{\mathrm{d}}} \cdot e^{-\frac{\Delta G^{\circ}_{\mathrm{fold}}}{RT}} + e^{-\frac{\Delta G^{\circ}_{\mathrm{fold}}}{RT}} + 1 \quad (6)$$

where $\Delta\Delta G_{\mathrm{balance}}$ represents the observed free energy difference; $\Delta G^{\circ}_{\mathrm{fold}}$ and K°_{d} denote the folding energy and binding constant, respectively. This approach allows accurate characterization of non-canonical structures including DNA triplexes, G-quadruplexes, and aptamers under native conditions.

To further demonstrate the capability of native characterization, Wu *et al.* used FESA to systematically study the folding and binding energies ($\Delta G^{\circ}_{\mathrm{fold}}$ and $\Delta G^{\circ}_{\mathrm{bind}}$) of the thrombin-binding aptamer (TBA) under various conditions, including different cations, molecular crowding, and cell-mimicking environments.[110] Na^+, NH_4^+, and Mg^{2+} had minimal effects, whereas K^+ and Sr^{2+} enhanced stability by up to -1.60 kcal mol^{-1}. Under molecular crowding (simulated using 20–40 wt% PEG200), crowding alone induced a stabilization of up to -1.48 kcal mol^{-1} in $\Delta G^{\circ}_{\mathrm{fold}}$, which was further enhanced to -4.57 kcal mol^{-1} in the presence of potassium. Similarly, the binding free energy strengthened from -9.34 to -10.86 kcal mol^{-1} under cell-mimicking conditions.

Beyond toehold exchange, conventional strand displacement reactions can also be engineered into actuation-responsive tools with reversible behavior. Traditionally, Mg^{2+} is required to screen electrostatic repulsion, guiding displacement through an S_N2-like pathway (Fig. 10a and b). However, Xu *et al.* showed that replacing Mg^{2+} with double-stranded DNA binders enables programmable control through an S_N1 type mechanism, in which the protecting strand is released first (Fig. 10c).[111] This binder-induced nucleic acid strand displacement (BIND) produces a "pseudo-reversible" signal pattern: an initial moderate signal from spontaneous denaturation (domain I), suppression at low binder concentrations due to duplex stabilization (domain II), and promotion of the S_N2 pathway at high binder concentrations (domains III and IV). By analyzing binding curves, it is possible to determine affinities, binding site sizes, cooperativity, and thermodynamic parameters (*via* the van't Hoff equation), demonstrating the potential of DNA nanotechnology for high-throughput screening of nucleic acid interactions.[112]

In summary, interactions involving nucleic acid–nucleic acid, aptamer–protein, and dsDNA-binder molecules can be effectively studied using DNA reaction-based molecular tools. A key step is constructing a reversible cycle that links the parameter of interest with a quantifiable strand displacement reaction. Both catalytic circuits and toehold-exchange systems can serve this purpose with fast kinetics. Another essential step is careful design of the reference system so that the reversible cycle responds specifically to the intended stimulus. Experimental parameters such as toehold length, GC content, and reactant stoichiometry can be finely adjusted to optimize the dynamic range.

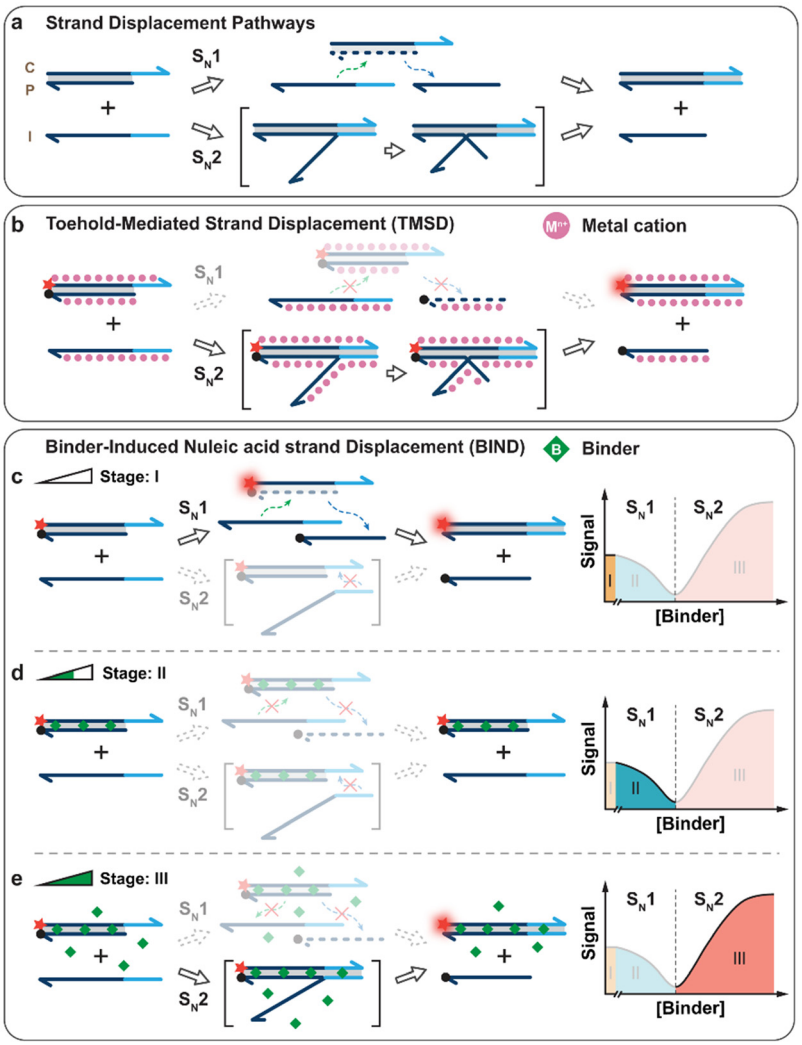

Fig. 10 (a) Schematic illustration of two possible reaction pathways (S_N1 and S_N2) for a typical toehold-mediated strand displacement reaction. (b) The conventional strand displacement reaction is dominated by the S_N2 reaction pathway, where metal cations help stabilize the triplex intermediate. (c) Activation of the S_N1 reaction pathway by preparing the displacement reaction in a buffer containing no or very low concentrations of metal ions, which is labeled as domain I in the BIND curve. (d) Inhibition of both reaction pathways in response to low concentrations of DNA binders in BIND, which is labeled as domain II in the BIND curve. Activation of the S_N2 reaction pathway in response to high concentrations of DNA binders in BIND, which is labeled as domain III in the BIND curve. Copyright 2023, Springer.

3.3. Direct hybridization-based molecular tools

In addition to constructing molecular tools through DNA-based reaction networks, a more direct though less versatile approach involves using well-designed strand hybridization systems. A representative example is the characterization of base-stacking energetics. Base-stacking interactions serve as the primary stabilizing force in double-stranded DNA, making their precise thermodynamic quantification a long-standing goal in nucleic acid research. Although extensive efforts were made through the 1990s to measure stacking free energies, significant discrepancies persisted between different experimental datasets.[113] This challenge arises from the difficulty of isolating individual base-stacking contributions from their structural context within the DNA helix. Early methods analyzed stabilization effects from flanking strands on duplexes with single-stranded overhangs (Fig. 11a),[114] but these measurements inherently combined stacking energies with dangling-end contributions. A major advance came in 2004 when Frank-Kamenetskii's research group developed a strategy to directly quantify stacking forces at DNA "nick" sites (Fig. 11b).[115,116]

This method exploits the thermodynamic equilibrium between two states in nicked DNA helices: an open conformation without base-stacking and a closed conformation with coaxial stacking across the nick (Fig. 11b). According to the Boltzmann distribution, the free energy can be determined from the population ratio of these two states.

$$\frac{N_{\text{closed}}}{N_{\text{open}}} = \exp\left(-\frac{\Delta G_{\text{stack}}}{RT}\right) \quad (7)$$

where T is the absolute temperature and R is the gas constant.

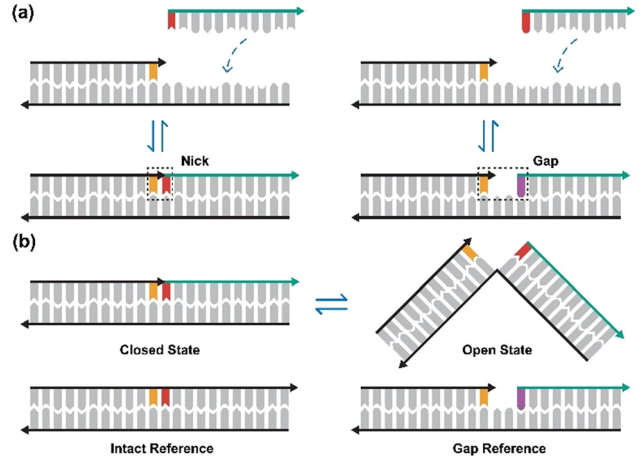

Fig. 11 Schematic demonstration of two approaches to measure the energetics of dinucleotide base-stacking.

To resolve these conformational populations experimentally, the team used polyacrylamide gel electrophoresis (PAGE) to distinguish stacked *versus* unstacked states. The structural discontinuity at the nick introduces a localized kink that alters electrophoretic mobility due to differences in helix rigidity. Fully double-stranded DNA and a gapped complex served as positive and negative controls, respectively, with at least two nucleotides required in the gap to ensure effective structure formation.[117]

Since conformational exchange occurs rapidly relative to equilibration in the gel matrix, only a single band was observed during electrophoresis. The overall mobility (μ) represented a population-weighted average of the absolute mobilities of the open (μ_{open}) and closed (μ_{closed}) conformations. Quantitative analysis was enhanced through urea-enhanced PAGE, where varying denaturant concentrations altered the mobility of the conformational mixture. Stacking free energies under physiological conditions (0 M urea) were then determined by linear extrapolation of the urea-dependent profiles.

$$\mu = \frac{N_{closed}}{N_{closed} + N_{open}}\mu_{closed} + \frac{N_{open}}{N_{closed} + N_{open}}\mu_{open} \quad (8)$$

Regrouping the above equation produced the relationship between population ratio and mobilities.

$$\frac{N_{closed}}{N_{open}} = \frac{\mu - \mu_{open}}{\mu_{closed} - \mu} \quad (9)$$

Using this approach, the researchers found the following order of stacking affinity: TG < AG < GA < GT. Additionally, for the same base pair combination, the stacking strength was largely independent of whether the nick was located on the forward (sense) or reverse (antisense) strand. For example, the free energy for 5′-G|A-3′ stacking was similar to that for 3′-C|T-5′. This method also enabled isothermal measurement of stacking free energies across a temperature range of 10–50 °C.

In subsequent studies, Frank-Kamenetskii and colleagues systematically characterized how DNA base-stacking free energies depend on temperature and ionic strength.[117] Their approach allowed the first experimental determination of stacking parameters through isothermal measurements over a broad temperature range without requiring extrapolation. The results confirmed that DNA stability is predominantly determined by stacking forces, which vary with both temperature and sodium ion concentration. Base pairing contributions were minimal: G:C pairs provided almost no stabilization, while A:T pairs even showed slight destabilization.

Beyond adjusting sequence length or temperature to fine-tune equilibrium, chemicals such as urea are commonly used to modulate duplex stability. Accurate thermodynamic characterization of DNA systems—particularly those involving non-canonical structures like G-quadruplexes, triplexes, or aptamer-ligand complexes—remains challenging due to limitations in prediction tools such as NUPACK and Mfold, which often fail to account for chemical modifications, environmental conditions, or complex tertiary structures. Traditional experimental methods like thermal melting curves, isothermal titration calorimetry, and binding assays also face limitations in sensitivity, cost, and applicability to weak interactions. To address these gaps, Vallée-Bélisle's group introduced urea titration as a versatile and precise method for determining folding and binding free energies of diverse DNA-based systems under native conditions (Fig. 12).[118]

This approach used DNA constructs including unimolecular structures (*e.g.*, stem-loop switches, G-quadruplexes, triplexes (Fig. 12a)) and bimolecular complexes (*e.g.*, DNA–DNA hybrids (Fig. 12b), aptamer-target pairs (Fig. 12c)), labeled with fluorophore-quencher pairs for fluorescence monitoring. Urea titration experiments involved gradually increasing urea concentration (0–10 M) in buffered solutions while tracking fluorescence changes. The resulting curves were fitted using two-state or three-state denaturation models to extract ΔG°, *m*-values (cooperativity parameters), and K_d. As a proof of concept, the authors determined folding free energies of unimolecular DNA structures assuming a two-state model (Fig. 12a). The cocaine-binding aptamer showed a folding free energy -1.7 ± 0.1 kcal mol^{-1} alone, which shifted to -4.8 ± 0.4 kcal mol^{-1} ($K_d \approx 302$ μM) upon cocaine saturation. This aligned with values from binding curves (-5.5 ± 0.3 kcal mol^{-1}), confirming the utility of urea titration for characterizing aptamer–ligand interactions. For stem-loop-based switches such as molecular beacons, urea curves revealed two transitions: target dissociation and switch unfolding (Fig. 12d). Binding free energies ranged from -11.5 to -14.5 kcal mol^{-1} depending on stem stability. A three-state model (eqn (7)) was used to fit the data, highlighting the competition between target binding and switch folding. Values derived from urea titration showed better accuracy than NUPACK predictions, which overestimated energies by approximately 6 kcal mol^{-1}.

Thus, this approach offers improved accuracy and applicability compared to traditional methods like thermal melting or binding curves. Although potential urea-ion interactions and

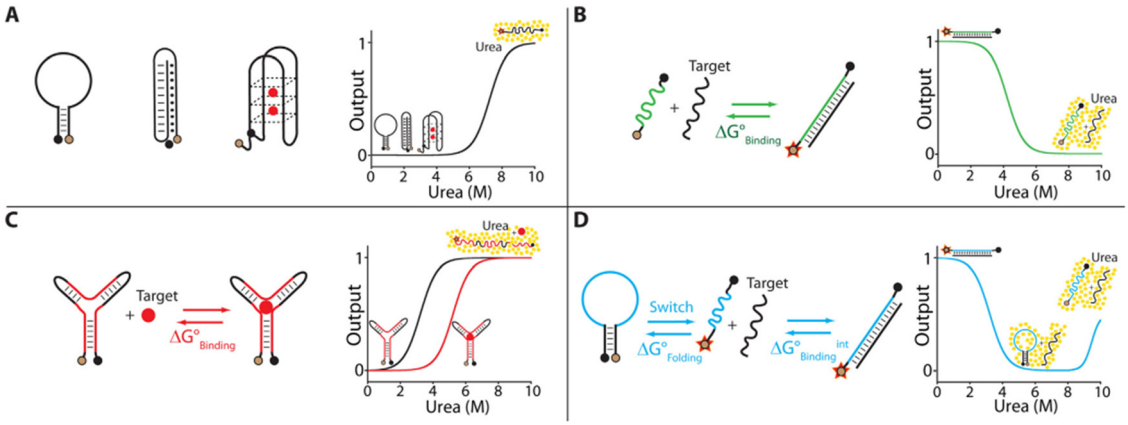

Fig. 12 Measuring the folding and binding free energies of DNA-based nanodevices and nanoswitches using urea titration curves.[118] (a) Determination of the folding free energy of DNA unimolecular structures (*e.g.*, stem–loop motifs). (b) Measurement of the binding free energy for DNA–DNA duplex formation. (c) Evaluation of the binding free energy between DNA aptamers and their non-DNA targets. (d) Determination of the binding free energy between DNA conformational nanoswitches and their DNA targets. Copyright 2017, Oxford University Press.

fitting assumptions require careful consideration, urea titration effectively bridges computational predictions and experimental validation, supporting the optimization of DNA-based nanodevices for sensing, computing, and drug delivery.

Another paradigm for using intramolecular conformational switching to measure thermodynamic parameters is the molecular clamp approach developed by Tom Soh and colleagues (Fig. 13a).[119] The DNA molecular clamp technique uses the mechanical properties of double-stranded DNA to apply controlled tension to target structures. In the initial study, a short dsDNA clamp was used to unfold aptamers under equilibrium conditions, enabling direct measurement of ΔG_{fold} through time-lapse gel electrophoresis and monomer–dimer equilibrium analysis. This method successfully determined the folding energy of the thrombin-binding aptamer HD22 (-10.40 kJ mol^{-1}) and a model hairpin structure (-9.05 kJ mol^{-1}), consistent with computational predictions and earlier estimates. In a subsequent study, Chung *et al.* extended this strategy to proteins, using a convertible ssDNA/dsDNA bridge to apply piconewton-scale forces on talin rod domains, inducing conformational changes that exposed cryptic binding sites for vinculin and ARPC5L (Fig. 13b).[120]

Key advantages of the DNA molecular clamp include operational simplicity, compatibility with standard laboratory equipment such

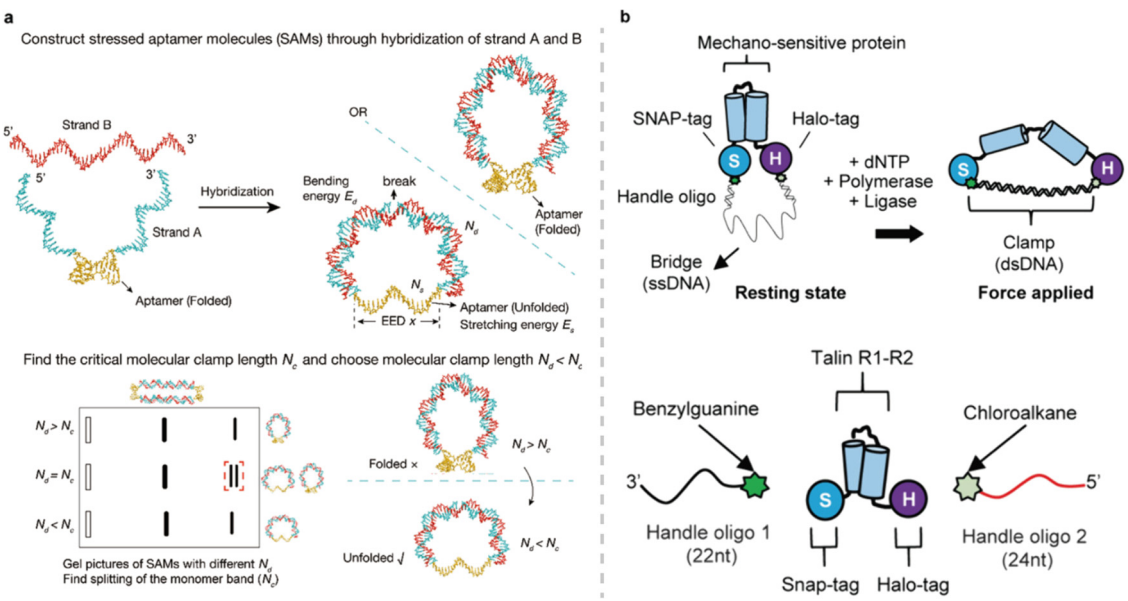

Fig. 13 Schematic illustrations of DNA-based molecular clamp strategies for quantifying molecular energetics and studying mechanobiology. (a) The folding energy measurement by molecular clamping (FE-MC) method for determining aptamer folding energy, where a short dsDNA clamp applies tension to unfold the nucleic acid structure.[119] Copyright 2020, American Chemical Society. (b) Application of a programmable DNA clamp to exert piconewton-scale forces on the Talin R1–R2 protein, enabling investigation of its force-dependent interactions with ligands such as vinculin D1 and ARPC5L.[120] Copyright 2024, American Chemical Society.

as gel electrophoresis, and applicability to diverse targets including nucleic acids and proteins. It enables direct, model-free quantification of thermodynamic parameters and offers tunability through variable clamp lengths. Limitations include force restrictions due to DNA buckling at extensions beyond ~30 nm, structural heterogeneity at higher tensions, and the need for empirical optimization of clamp length for different targets. Although the method accesses physiological force ranges (1–7 pN), its precision depends on accurate fitting of reaction-diffusion models and assumes minimal nonspecific interactions. Despite these challenges, the DNA molecular clamp represents a versatile and accessible tool for probing mechanobiology and biomolecular stability.

Recently, Lyu's group introduced an equilibrium-based Metastable DNA Reference Calorimetry (MDRC) method for precise thermodynamic characterization of aptamer-target interactions. This approach uses metastable DNA hybridization probes to reduce measurement deviations that have historically affected fluorescence-based methods.[121] By converting the aptamer binding equilibrium into a DNA hybridization reference system, MDRC enables direct calculation of key thermodynamic parameters—including K_d, ΔG°, ΔH°, and ΔS°, through high-throughput fluorescence detection. The authors developed tailored algorithms for various binding models and successfully applied MDRC to aptamers with one or multiple binding sites for small molecules (*e.g.*, ATP), proteins (*e.g.*, thrombin), and whole cells. A key finding was that for the ATP aptamer with two binding sites, binding of the first molecule negatively influences affinity for the second, an effect that is temperature-dependent and leads to complete loss of secondary binding at higher temperatures.

The main advantage of MDRC is its ability to minimize quantification errors inherent in ITC or SPR, providing more reliable and comparable thermodynamic data across different aptamer systems. Its compatibility with standard laboratory equipment and capacity for high-throughput analysis enhance its accessibility. However, the method's effectiveness depends on careful design of metastable DNA probes, as deviations can occur if hybridization is either too stable or too unstable. Additionally, while MDRC shows broad applicability, its performance in complex biological matrices may require further optimization to account for nonspecific interactions. Despite these limitations, MDRC represents a significant advance for standardized evaluation of aptamer binding energetics, supporting improved design of aptamer-based probes, therapeutics, and nanodevices.

In summary, direct hybridization-based molecular tools offer a versatile strategy for investigating molecular interactions. Rather than designing reversible circuits that directly respond to biochemical stimuli, hybridization tools function as molecular rulers with well-defined thermodynamic references. These approaches leverage the predictable base-pairing properties of nucleic acids to generate reproducible, sequence-dependent energy landscapes, making them particularly suitable for measuring aptamer stability, protein-DNA interactions, and allosteric switching behaviors under equilibrium conditions.

3.4. DNA origami-based molecular tools

DNA origami is an innovative nanotechnology that enables the precise folding of DNA into customized two- or three-dimensional nanostructures through programmable Watson–Crick base pairing. First introduced by Paul Rothemund in 2006, this method uses a long single-stranded DNA scaffold (typically derived from the M13 bacteriophage) along with hundreds of short synthetic "staple" strands. These staples bind to specific regions of the scaffold, guiding its folding into defined shapes such as geometric patterns, tubes, or complex nanoscale devices. The assembly occurs autonomously under controlled thermodynamic conditions, producing structures with high precision and addressable functional sites.

Recent progress in single-molecule biophysics has utilized structural DNA nanotechnology to study intermolecular interactions. In a notable study by Kilchherr *et al.*,[122] researchers constructed nanoscale DNA beam assemblies connected by a flexible polymer tether to quantitatively measure blunt-end stacking forces. To improve detection sensitivity for these weak interactions, the design incorporated multivalent parallel helix bundles that amplified stacking through cooperative effects (Fig. 14). Structural analysis revealed different thermodynamic behaviors between nick-site and blunt-end stacking, attributed to the structural constraints imposed by nicks in the DNA helix. The programmed assembly of aligned DNA beams was confirmed using transmission electron microscopy (TEM) and gel electrophoresis. The team further characterized stacking interaction kinetics *via* single-molecule fluorescence lifetime measurements, establishing a systematic profile for all 16 possible nucleobase stacking combinations.

DNA-based points accumulation for imaging in nanoscale topography (DNA-PAINT) offers another approach for determining fundamental thermodynamic parameters of nucleic acids.[123] In a study by Banerjee *et al.*, base-stacking energetics were quantified at high-throughput single-molecule resolution using multiplexed DNA-PAINT microscopy.[124] This technique uses transient hybridization between dye-labeled imager

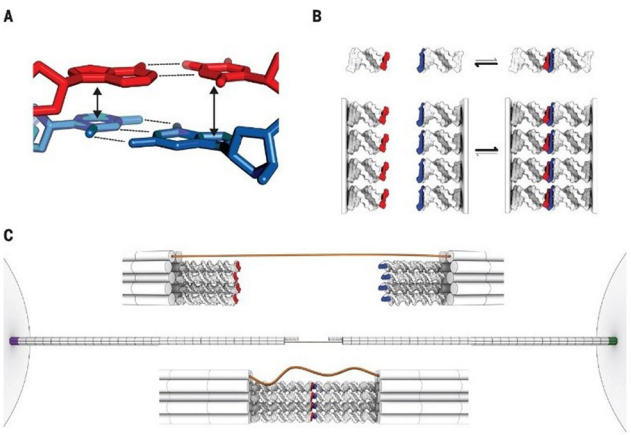

Fig. 14 Schematic illustration of the design of DNA origami beams and interaction of blunt-ends.[122] Copyright 2016, The American Association for the Advancement of Science.

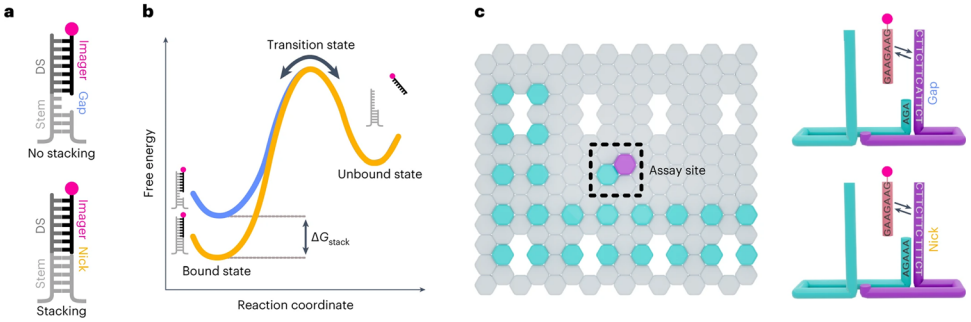

Fig. 15 (a) Two imager strands that form nick (stacking) and gap (unstack) configurations with the docking strand. (b) Representative free-energy diagram of the bound and unbound states. (c) Graphical representation of the origami layout, where the L-shaped grid with cyan-colour labels is used for identifying the locations of origami structures, and the docking site with magenta colour label is for probing base-stacking interactions.[124] Copyright 2023, Springer.

strands and surface-anchored docking strands, where terminal base-stacking interactions extend the binding dwell time and reflect complex stability (Fig. 15a and b). DNA origami nanoarrays served as programmable platforms, with spatially arranged docking strands enabling systematic analysis of all canonical base-stacking variants (Fig. 15c). Thermodynamic parameters were obtained by comparing binding kinetics between stacked (nick-imager) and unstacked (gap-imager) configurations (eqn (10)–(13)).

The observed apparent dissociation rate from the bound state ($k_{off,app}$) can be written as:

$$k_{off,app} = \left(\frac{N_{st}}{N_{st} + N_{unst}}\right) \cdot k_{off,st} + \left(\frac{N_{unst}}{N_{st} + N_{unst}}\right) \cdot k_{off,unst} \quad (10)$$

where $k_{off,st}$ and $k_{off,unst}$ are the dissociation rates for stacked and unstacked states, respectively. N_{st} and N_{unst} are the occupancies of stacked and unstacked states during the bound state.

By regrouping the equation and assuming $k_{off,st}$ was very slow compared to $k_{off,app}$, the relationship between observed configuration occupancies and kinetic rates was:

$$\frac{N_{st}}{N_{unst}} = \frac{k_{off,unst} - k_{off,app}}{k_{off,app}} \quad (11)$$

where the $k_{off,unst}$ can be measured by using a gapped imager strand, hence:

$$\frac{N_{st}}{N_{unst}} = \frac{k_{off,gap} - k_{off,app}}{k_{off,app}} \quad (12)$$

According to the equilibrium equation, the stacking free energy can be derived as:

$$\Delta G_{stack} = -kT \ln\left(\frac{N_{st}}{N_{unst}}\right) = kT \ln\left(\frac{k_{off,gap} - k_{off,app}}{k_{off,app}}\right) \quad (13)$$

As such, all 16 possible dinucleotide stacking energetics were systematically determined according to above equation.

In summary, DNA origami has become a powerful platform for quantitatively studying molecular interactions with nanoscale precision. Its programmable design allows accurate placement of biological ligands and probes with controlled geometry and valency. The ability to engineer spatial organization and multivalency further enables investigation of complex mechanisms such as receptor activation thresholds and enzymatic cascade efficiency, which are essential for understanding signaling pathways and designing therapeutic nanodevices. Recent improvements in purification and characterization methods (including electrophoresis, microscopy, and spectroscopy) ensure the reliability and reproducibility of functionalized nanostructures, offering robust systems for high-resolution mapping of molecular binding events. These features establish DNA origami as a versatile tool in nanobiotechnology, providing unique insights into interaction dynamics relevant to biological function and disease.

4. Challenges & future perspectives

This review briefly surveys diverse methodologies for quantitatively characterizing interactions between nucleic acids and other molecules. Conventional methods such as ITC directly measure thermodynamic parameters of binding processes, yet impose relatively high demands on sample concentration and quantity, while offering limited resolution in complex systems. Surface-based methods including SPR and BLI enable real-time monitoring of binding kinetics; however, the required immobilization steps may alter the native conformation and activity of the molecules. Although these established methods have provided a crucial foundation for studying nucleic acid interactions, recently developed programmable nucleic acid-based strategies offer distinct advantages. Leveraging the programmable nature of nucleic acids, these approaches enable precise control and quantitative analysis of reaction driving forces, rates, and competitive pathways at the molecular level.[125–127] They effectively address limitations of conventional methods in mimicking physiological conditions and characterizing weak interactions, thereby offering new experimental pathways to elucidate nucleic acid interaction mechanisms under near-native biological conditions and to establish accurate kinetic models. Looking ahead, nucleic acid based molecular tools are expected to move beyond the study of nucleic acid interactions

themselves. Due to their structural programmability and biocompatibility, DNA and RNA nanostructures have the potential to serve as universal quantitative probes for studying protein–protein interactions, protein small molecule interactions, and complex system interactions. However, this field still faces many challenges. First, the quantitative relationship between structural design and thermodynamic output has not been fully established. Second, the strong sensitivity of the system to environmental factors such as ionic strength, molecular crowding, and temperature can affect measurement accuracy. If these problems can be solved, nucleic acid molecular tools will evolve from theoretical models into experimental platforms that can be used to quantitatively describe intracellular interaction networks, providing key support for cross scale research from the molecular level to systems biology.

Conflicts of interest

There are no conflicts to declare.

Abbreviations

FP	Fluorescence polarization
FA	Fluorescence anisotropy
FRET	Förster resonance energy transfer
BRET	Bioluminescence resonance energy transfer
FCS	Fluorescence correlation spectroscopy
CD	Circular dichroism
MS	Mass spectrometry
NMR	Nuclear magnetic resonance
K_d	Dissociation constant
trFRET	Time-resolved FRET
smFRET	Single-molecule FRET
kinFRET	Kinetics FRET
SpS	Spectral shift
EMSA	Electrophoretic mobility shift assay
ACE	Affinity capillary electrophoresis
KCE	Kinetic capillary electrophoresis
MST	Microscale thermophoresis
FFF	Field-flow fractionation
BANC-seq	Binding Affinities to Native Chromatin by Sequencing
CE-SELEX	Capillary electrophoresis-based systematic evolution of ligands by exponential enrichment
k_{on}	Rates of association
k_{off}	Rates of dissociation
T	Temperature
ΔH	Enthalpy change
ΔS	Entropy change
ITC	Isothermal titration calorimetry
DSC	Differential scanning calorimetry
n	Stoichiometry
N	Occupancy
T_m	Melting temperature
SPR	Surface plasmon resonance
BLI	Bio-layer interferometry
QCM	Quartz crystal microbalance
FAIVE	Functional Aptamers *in vitro* Evolution
FACS	Fluorescence-activated cell sorting
Δf	Frequency shift
OT	Optical tweezers
MT	Magnetic tweezers
AFM	Atomic force microscopy
TPM	Tethered particle motion
SNVs	Single nucleotide variants
ΔG°	Standard Gibbs free energy change
ΔH°	Standard enthalpy change
ΔS°	Standard entropy change
TEEM	Toehold exchange energy measurement
HRM	High-resolution melting
FESA	Free energy shift assay
TBA	Thrombin-binding aptamer
BIND	Binder-induced nucleic acid strand displacement
PAGE	Polyacrylamide gel electrophoresis
μ	Mobility
FE-MC	The folding energy measurement by molecular clamping
MDRC	Metastable DNA Reference Calorimetry
TEM	Transmission electron microscopy

Data availability

No primary research results, software, nor code have been included, and no new data were generated nor analysed as part of this review.

Acknowledgements

This work was supported by the National Key R&D Program of China (2024YFA1209401), the National Natural Science Foundation of China (22574114, 22074099, 22204112), the China Postdoctoral Science Foundation (2023M732423), and the Sichuan Science and Technology Program (2025NSFJQ0038).

References

1 H. Zhang, Y. Tang, S.-J. Lee, Z. Wei, J. Cao and C. C. Richardson, Binding Affinities among DNA Helicase-Primase, DNA Polymerase, and Replication Intermediates in the Replisome of Bacteriophage T7, *J. Biol. Chem.*, 2016, **291**(3), 1472–1480, DOI: 10.1074/jbc.m115.698233.

2 J. N. K. Quartey and D. J. Goss, eIF3d and eIF4G2 Mediate an Alternative Mechanism of Cap-Dependent but eIF4E-Independent Translation Initiation, *J. Biol. Chem.*, 2025, **301**(4), 108317, DOI: 10.1016/j.jbc.2025.108317.

3 F. Jacob and J. Monod, Genetic Regulatory Mechanisms in the Synthesis of Proteins, *J. Mol. Biol.*, 1961, **3**(3), 318–356, DOI: 10.1016/S0022-2836(61)80072-7.

4 J. D. Richards, K. A. Johnson, H. Liu, A.-M. McRobbie, S. McMahon, M. Oke, L. Carter, J. H. Naismith and M. F.

White, Structure of the DNA Repair Helicase Hel308 Reveals DNA Binding and Autoinhibitory Domains*, *J. Biol. Chem.*, 2008, **283**(8), 5118–5126, DOI: 10.1074/jbc.m707548200.

5 Z. Wang, C. Zhang, S. He and D. Xu, An Ultrasensitive Fluorescence Aptasensor for SARS-CoV-2 Antigen Based on Hyperbranched Rolling Circle Amplification, *Talanta*, 2023, **255**, 124221, DOI: 10.1016/j.talanta.2022.124221.

6 G. E. Vezeau, L. R. Gadila and H. M. Salis, Automated Design of Protein-Binding Riboswitches for Sensing Human Biomarkers in a Cell-Free Expression System, *Nat. Commun.*, 2023, **14**(1), 2416, DOI: 10.1038/s41467-023-38098-0.

7 Y. Mou, P. Yin, M. Chen, C. Wei, Y. Zhang, J. Zhang, Y. Zhao, X. Luo and Y. Wang, Engineering of An Aptamer-Functionalized Fluorescent DNA Sensor for Cu(II) Responding in Living Tumor Cells, *Anal. Chem.*, 2023, **95**(21), 8348–8356, DOI: 10.1021/acs.analchem.3c01008.

8 M. Altai, Á. Nagy, P. Granit, W. Zedan, M. Cerezo-Magaña, J. Park, K. Lückerath, S. Geres, M. Sydoff, D. L. J. Thorek, K. Westerlund, D. Ulmert and A. E. Karlström, Optimizing Peptide Nucleic Acid-Based Pretargeting for Enhanced Targeted Radionuclide Therapy, *J. Controlled Release*, 2025, **381**, 113551, DOI: 10.1016/j.jconrel.2025.02.047.

9 M. Yang, C. Li, G. Ye, C. Shen, H. Shi, L. Zhong, Y. Tian, M. Zhao, P. Wu, A. Hussain, T. Zhang, H. Yang, J. Yang, Y. Weng, X. Liu, Z. Wang, L. Gan, Q. Zhang, Y. Liu, G. Yang, Y. Huang and Y. Zhao, Aptamers Targeting SARS-CoV-2 Nucleocapsid Protein Exhibit Potential Anti Pan-Coronavirus Activity, *Signal Transduct. Target. Ther.*, 2024, **9**(1), 40, DOI: 10.1038/s41392-024-01748-w.

10 R. Ye, H. Zhao, X. Wang and Y. Xue, Technological Advancements in Deciphering RNA-RNA Interactions, *Mol. Cell*, 2024, **84**(19), 3722–3736, DOI: 10.1016/j.molcel.2024.06.036.

11 R. A. C. Ferraz, A. L. G. Lopes, J. A. F. da Silva, D. F. V. Moreira, M. J. N. Ferreira and S. V. de Almeida Coimbra, DNA–Protein Interaction Studies: A Historical and Comparative Analysis, *Plant Methods*, 2021, **17**(1), 82, DOI: 10.1186/s13007-021-00780-z.

12 S. Chen, Q. Mao, H. Cheng and W. Tai, RNA-Binding Small Molecules in Drug Discovery and Delivery: An Overview from Fundamentals, *J. Med. Chem.*, 2024, **67**(18), 16002–16017, DOI: 10.1021/acs.jmedchem.4c01330.

13 S. R. Eisen, P. Dauphin-Ducharme and P. E. Johnson, Solution-Based Biophysical Characterization of Conformation Change in Structure-Switching Aptamers, *Q. Rev. Biophys.*, 2024, **57**, e9, DOI: 10.1017/S0033583524000076.

14 A. T. H. Le, S. M. Krylova, S. S. Beloborodov, T. Y. Wang, R. Hili, P. E. Johnson, F. Li, R. N. Veedu, S. Belyanskaya and S. N. Krylov, How to Develop and Prove High-Efficiency Selection of Ligands from Oligonucleotide Libraries: A Universal Framework for Aptamers and DNA-Encoded Small-Molecule Ligands, *Anal. Chem.*, 2021, **93**(13), 5343–5354, DOI: 10.1021/acs.analchem.1c00601.

15 R. Thevendran and M. Citartan, Assays to Estimate the Binding Affinity of Aptamers, *Talanta*, 2022, **238**, 122971, DOI: 10.1016/j.talanta.2021.122971.

16 X. A. Feng, M. F. Poyton and T. Ha, Multicolor Single-Molecule FRET for DNA and RNA Processes, *Curr. Opin. Struct. Biol.*, 2021, **70**, 26–33, DOI: 10.1016/j.sbi.2021.03.005.

17 C. J. Bustamante, Y. R. Chemla, S. Liu and M. D. Wang, Optical Tweezers in Single-Molecule Biophysics, *Nat. Rev. Methods Primer*, 2021, **1**(1), 25, DOI: 10.1038/s43586-021-00021-6.

18 A. Kopūstas, M. Zaremba and M. Tutkus, DNA Flow-Stretch Assays for Studies of Protein-DNA Interactions at the Single-Molecule Level, *Appl. Nano*, 2022, **3**(1), 16–41, DOI: 10.3390/applnano3010002.

19 M. Filius, L. Fasching, R. van Wee, A. Y. Rwei and C. Joo, Decoding Aptamer-Protein Binding Kinetics for Continuous Biosensing Using Single-Molecule Techniques, *Sci. Adv.*, 2025, **11**(7), eads9687, DOI: 10.1126/sciadv.ads9687.

20 M. D. Baaske, M. R. Foreman and F. Vollmer, Single-Molecule Nucleic Acid Interactions Monitored on a Label-Free Microcavity Biosensor Platform, *Nat. Nanotechnol.*, 2014, **9**(11), 933–939, DOI: 10.1038/nnano.2014.180.

21 B. Yurke, A. J. Turberfield, A. P. Mills, F. C. Simmel and J. L. Neumann, A DNA-Fuelled Molecular Machine Made of DNA, *Nature*, 2000, **406**(6796), 605–608, DOI: 10.1038/35020524.

22 C. Wang, J. H. Bae and D. Y. Zhang, Native Characterization of Nucleic Acid Motif Thermodynamics via Non-Covalent Catalysis, *Nat. Commun.*, 2016, **7**(1), 10319, DOI: 10.1038/ncomms10319.

23 D. Huang, Y. Liu, G. A. Wang, S. Lv, Y. Tan and F. Li, Chemical tools for discriminating single nucleotide variants: from design principles to clinical applications, *Chem. Soc. Rev.*, 2025, DOI: 10.1039/D5CS01006C.

24 P. Karthik, P. A. Jose, A. Chellakannu, S. Gurusamy, P. Ananthappan, R. Karuppathevan, V. S. Vasantha, J. Rajesh, S. Ravichandran and M. Sankarganesh, Green Synthesis of MnO2 Nanoparticles from Psidium Guajava Leaf Extract: Morphological Characterization, Photocatalytic and DNA/BSA Interaction Studies, *Int. J. Biol. Macromol.*, 2024, **258**, 128869, DOI: 10.1016/j.ijbiomac.2023.128869.

25 A. Langer, A. Lüdecke, T. Bartoschik, Q. Cehlar, S. Duhr, P. Baaske and W. Streicher, A New Spectral Shift-Based Method to Characterize Molecular Interactions, *Assay Drug Dev. Technol.*, 2022, **20**(2), 83–94, DOI: 10.1089/adt.2021.133.

26 Q. Zhao, J. Tao, W. Feng, J. S. Uppal, H. Peng and X. C. Le, Aptamer Binding Assays and Molecular Interaction Studies Using Fluorescence Anisotropy - A Review, *Anal. Chim. Acta*, 2020, **1125**, 267–278, DOI: 10.1016/j.aca.2020.05.061.

27 A. M. Rossi and C. W. Taylor, Analysis of Protein-Ligand Interactions by Fluorescence Polarization, *Nat. Protoc.*, 2011, **6**(3), 365–387, DOI: 10.1038/nprot.2011.305.

28 A. V. Samokhvalov, O. G. Maksimenko, S. A. Eremin, A. V. Zherdev and B. B. Dzantiev, Interactions of Ligand, Aptamer, and Complementary Oligonucleotide: Studying Impacts of Na+ and Mg2+ Cations on Sensitive FRET-Based Detection of Aflatoxin B1, *Molecules*, 2025, **30**(10), 2125, DOI: 10.3390/molecules30102125.

29 T. A. Vickers and S. T. Crooke, Development of a Quantitative BRET Affinity Assay for Nucleic Acid-Protein Interactions, *PLoS One*, 2016, **11**(8), e0161930, DOI: 10.1371/journal.pone.0161930.
30 D. Porciani, M. M. Alampi, S. Abbruzzetti, C. Viappiani and P. Delcanale, Fluorescence Correlation Spectroscopy as a Versatile Method to Define Aptamer–Protein Interactions with Single-Molecule Sensitivity, *Anal. Chem.*, 2024, **96**(1), 137–144, DOI: 10.1021/acs.analchem.3c03341.
31 M. Marušič, M. Toplishek and J. Plavec, NMR of RNA - Structure and Interactions, *Curr. Opin. Struct. Biol.*, 2023, **79**, 102532, DOI: 10.1016/j.sbi.2023.102532.
32 M. M. Makowski, C. Gräwe, B. M. Foster, N. V. Nguyen, T. Bartke and M. Vermeulen, Global Profiling of Protein–DNA and Protein–Nucleosome Binding Affinities Using Quantitative Mass Spectrometry, *Nat. Commun.*, 2018, **9**(1), 1653, DOI: 10.1038/s41467-018-04084-0.
33 H. Welte, P. Sinn and M. Kovermann, Fluorine NMR Spectroscopy Enables to Quantify the Affinity Between DNA and Proteins in Cell Lysate, *ChemBioChem*, 2021, **22**(20), 2973–2980, DOI: 10.1002/cbic.202100304.
34 D. M. Jameson and J. A. Ross, Fluorescence Polarization/Anisotropy in Diagnostics and Imaging, *Chem. Rev.*, 2010, **110**(5), 2685–2708, DOI: 10.1021/cr900267p.
35 V. LeTilly and C. A. Royer, Fluorescence Anisotropy Assays Implicate Protein-Protein Interactions in Regulating Trp Repressor DNA Binding, *Biochemistry*, 1993, **32**(30), 7753–7758, DOI: 10.1021/bi00081a021.
36 C. Bou-Nader, A. Bothra, D. N. Garboczi, S. H. Leppla and J. Zhang, Structural Basis of R-Loop Recognition by the S9.6 Monoclonal Antibody, *Nat. Commun.*, 2022, **13**(1), 1641, DOI: 10.1038/s41467-022-29187-7.
37 G. W. Gordon, G. Berry, X. H. Liang, B. Levine and B. Herman, Quantitative Fluorescence Resonance Energy Transfer Measurements Using Fluorescence Microscopy, *Biophys. J.*, 1998, **74**(5), 2702–2713, DOI: 10.1016/S0006-3495(98)77976-7.
38 R. A. Higuera-Rodriguez, M. C. De Pascali, M. Aziz, M. Sattler, U. Rant and W. Kaiser, Kinetic FRET Assay to Measure Binding-Induced Conformational Changes of Nucleic Acids, *ACS Sens.*, 2023, **8**(12), 4597–4606, DOI: 10.1021/acssensors.3c01527.
39 K. J. L. Zimmer, R. E. Johnson, H. Little, J. Duhamel and R. A. Manderville, Harnessing a Fluorescent Nucleobase Surrogate for Supramolecular FRET-Aptamer Detection and Target-Site Mapping, *ACS Sens.*, 2025, **10**(3), 1822–1832, DOI: 10.1021/acssensors.4c02772.
40 Y. Liu, O. Raymond and J. M. Hodgkiss, Exploring Fluorescence Spectral Shifts in Aptamer-Intercalating Cyanine Dye Complexes upon Binding to Specific Small Molecules, *ACS Sens.*, 2025, **10**(3), 2266–2275, DOI: 10.1021/acssensors.4c03579.
41 Y. Wu, Q. Yang, G. A. Wang and F. Li, Native Measurement of Aptamer Folding and Binding Energies Using a Free Energy Shift Assay, *JACS Au*, 2025, **5**(7), 3632–3638, DOI: 10.1021/jacsau.5c00689.
42 H. Yu, O. Alkhamis, J. Canoura, Y. Liu and Y. Xiao, Advances and Challenges in Small-Molecule DNA Aptamer Isolation, Characterization, and Sensor Development, *Angew. Chem., Int. Ed.*, 2021, **60**(31), 16800–16823, DOI: 10.1002/anie.202008663.
43 S. Stangherlin, Y. Ding and J. Liu, Dissociation Constant (Kd) Measurement for Small-Molecule Binding Aptamers: Homogeneous Assay Methods and Critical Evaluations, *Small Methods*, 2025, **9**(6), 2401572, DOI: 10.1002/smtd.202401572.
44 S. Slavkovic, Y. Zhu, Z. R. Churcher, A. A. Shoara, A. E. Johnson and P. E. Johnson, Thermodynamic Analysis of Cooperative Ligand Binding by the ATP-Binding DNA Aptamer Indicates a Population-Shift Binding Mechanism, *Sci. Rep.*, 2020, **10**(1), 18944, DOI: 10.1038/s41598-020-76002-8.
45 R. Helwa and J. D. Hoheisel, Analysis of DNA–Protein Interactions: From Nitrocellulose Filter Binding Assays to Microarray Studies, *Anal. Bioanal. Chem.*, 2010, **398**(6), 2551–2561, DOI: 10.1007/s00216-010-4096-7.
46 L. M. Hellman and M. G. Fried, Electrophoretic Mobility Shift Assay (EMSA) for Detecting Protein–Nucleic Acid Interactions, *Nat. Protoc.*, 2007, **2**(8), 1849–1861, DOI: 10.1038/nprot.2007.249.
47 F. Yu, Q. Zhao, D. Zhang, Z. Yuan and H. Wang, Affinity Interactions by Capillary Electrophoresis: Binding, Separation, and Detection, *Anal. Chem.*, 2019, **91**(1), 372–387, DOI: 10.1021/acs.analchem.8b04741.
48 C. J. Wienken, P. Baaske, U. Rothbauer, D. Braun and S. Duhr, Protein-Binding Assays in Biological Liquids Using Microscale Thermophoresis, *Nat. Commun.*, 2010, **1**(1), 100, DOI: 10.1038/ncomms1093.
49 J. C. Ferreon, N. Kongchan, P. S. Tsoi, K.-J. Choi, S. Kenrick, J. Neilson and A. C. M. Ferreon, Multivalent Protein–Nucleic Acid Interactions Probed by Composition-Gradient Multiangle Light Scattering, *ACS Omega*, 2024, **9**(39), 41003–41010, DOI: 10.1021/acsomega.4c06358.
50 M. Gilar, C. Doneanu and M. M. Gaye, Liquid Chromatography Methods for Analysis of mRNA Poly(A) Tail Length and Heterogeneity, *Anal. Chem.*, 2023, **95**(38), 14308–14316, DOI: 10.1021/acs.analchem.3c02552.
51 X. Lin, Y. Huang, J. Huang, H. Yuan, Y. Luo, Z. Lu, Y. Ao, J. Huang, S.-B. Chen, Z. Miao and L. Huang, From Theophylline to Adenine or preQ1: Repurposing a DNA Aptamer Revealed by Crystal Structure Analysis, *Angew. Chem., Int. Ed.*, 2025, **64**(22), e202504107, DOI: 10.1002/anie.202504107.
52 C. Qu and H. Du, Advance Technologies for DNA-Protein Interactions and Future Research Prospect, *Crop Des*, 2025, **4**(1), 100082, DOI: 10.1016/j.cropd.2024.100082.
53 C. M. Ouimet, C. I. D'amico and R. T. Kennedy, Advances in Capillary Electrophoresis and the Implications for Drug Discovery, *Expert Opin. Drug Discovery*, 2017, **12**(2), 213–224, DOI: 10.1080/17460441.2017.1268121.
54 A. Petrov, V. Okhonin, M. Berezovski and S. N. Krylov, Kinetic Capillary Electrophoresis (KCE): A Conceptual

Platform for Kinetic Homogeneous Affinity Methods, *J. Am. Chem. Soc.*, 2005, **127**(48), 17104–17110, DOI: 10.1021/ja056232l.

55 I. O. Neaga, E. Bodoki, S. Hambye, B. Blankert and R. Oprean, Study of Nucleic Acid–Ligand Interactions by Capillary Electrophoretic Techniques: A Review, *Talanta*, 2016, **148**, 247–256, DOI: 10.1016/j.talanta.2015.10.077.

56 E. Mitsuno, T. Endo, H. Hisamoto and K. Sueyoshi, Evaluation of the Interactions between Oligonucleotides and Small Molecules by Partial Filling–Nonequilibrium Affinity Capillary Electrophoresis, *Anal. Sci.*, 2022, **38**(6), 851–859, DOI: 10.1007/s44211-022-00101-x.

57 A. Jug, T. Bratkovič and J. Ilaš, Biolayer Interferometry and Its Applications in Drug Discovery and Development, *TrAC, Trends Anal. Chem.*, 2024, **176**, 117741, DOI: 10.1016/j.trac.2024.117741.

58 H. K. Neikes, K. W. Kliza, C. Gräwe, R. A. Wester, P. W. T. C. Jansen, L. A. Lamers, M. P. Baltissen, S. J. van Heeringen, C. Logie, S. A. Teichmann, R. G. H. Lindeboom and M. Vermeulen, Quantification of Absolute Transcription Factor Binding Affinities in the Native Chromatin Context Using BANC-Seq, *Nat. Biotechnol.*, 2023, **41**(12), 1801–1809, DOI: 10.1038/s41587-023-01715-w.

59 R. A. Wester, H. K. Neikes, R. G. H. Lindeboom and M. Vermeulen, Quantifying Genome-Wide Transcription Factor Binding Affinities for Chromatin Using BANC-Seq, *Nat. Protoc.*, 2024, **19**(12), 3590–3612, DOI: 10.1038/s41596-024-01026-7.

60 M. Bastos, O. Abian, C. M. Johnson, F. Ferreira-da-Silva, S. Vega, A. Jimenez-Alesanco, D. Ortega-Alarcon and A. Velazquez-Campoy, Isothermal Titration Calorimetry, *Nat. Rev. Methods Primer*, 2023, **3**(1), 1–23, DOI: 10.1038/s43586-023-00199-x.

61 T. Sakamoto, E. Ennifar and Y. Nakamura, Thermodynamic Study of Aptamers Binding to Their Target Proteins, *Biochimie*, 2018, **145**, 91–97, DOI: 10.1016/j.biochi.2017.10.010.

62 D. Burnouf, E. Ennifar, S. Guedich, B. Puffer, G. Hoffmann, G. Bec, F. Disdier, M. Baltzinger and P. Dumas, kinITC: A New Method for Obtaining Joint Thermodynamic and Kinetic Data by Isothermal Titration Calorimetry, *J. Am. Chem. Soc.*, 2012, **134**(1), 559–565, DOI: 10.1021/ja209057d.

63 W. B. Turnbull and A. H. Daranas, On the Value of c: Can Low Affinity Systems Be Studied by Isothermal Titration Calorimetry?, *J. Am. Chem. Soc.*, 2003, **125**(48), 14859–14866, DOI: 10.1021/ja036166s.

64 A. Velazquez-Campoy and E. Freire, Isothermal Titration Calorimetry to Determine Association Constants for High-Affinity Ligands, *Nat. Protoc.*, 2006, **1**(1), 186–191, DOI: 10.1038/nprot.2006.28.

65 L. Zhang, C. Batters, S. Aibara, Y. Gordiyenko, K. Žumer, J. Schmitzová, K. Maier, P. Cramer and S. Zhang, Structure of a Transcribing Pol II-DSIF-SPT6-U1 snRNP Complex, *Nat. Commun.*, 2025, **16**(1), 5823, DOI: 10.1038/s41467-025-60979-9.

66 F. Manyanga, Use of Differential Scanning Calorimetry (DSC) to Study the Thermodynamics of DNA-Based Interactions and Nucleic Acid-Based Therapeutics, *J. Anal. Pharm. Res.*, 2016, **2**(2), 00013, DOI: 10.15406/japlr.2016.02.00013.

67 R. W. Harkness, S. Slavkovic, P. E. Johnson and A. K. Mittermaier, Rapid Characterization of Folding and Binding Interactions with Thermolabile Ligands by DSC, *Chem. Commun.*, 2016, **52**(92), 13471–13474, DOI: 10.1039/C6CC05576A.

68 P. Wityk, R. Piątek, R. Nowak and D. Kostrzewa-Nowak, Generation and Characterization of a DNA-GCN4 Oligonucleotide-Peptide Conjugate: The Impact DNA/Protein Interactions on the Sensitization of DNA, *Molecules*, 2020, **25**(16), 3630, DOI: 10.3390/molecules25163630.

69 W. D. Wilson, Analyzing Biomolecular Interactions, *Science*, 2002, **295**(5562), 2103–2105, DOI: 10.1126/science.295.5562.2103.

70 T. M. Davis and W. D. Wilson, Determination of the Refractive Index Increments of Small Molecules for Correction of Surface Plasmon Resonance Data, *Anal. Biochem.*, 2000, **284**(2), 348–353, DOI: 10.1006/abio.2000.4726.

71 Y. Liu and W. D. Wilson, Quantitative Analysis of Small Molecule–Nucleic Acid Interactions with a Biosensor Surface and Surface Plasmon Resonance Detection, *In Drug-DNA Interaction Protocols*, ed K. R. Fox, Humana Press, Totowa, NJ, 2010, pp. 1–23. , DOI: 10.1007/978-1-60327-418-0_1.

72 B. Nguyen, F. A. Tanious and W. D. Wilson, Biosensor-Surface Plasmon Resonance: Quantitative Analysis of Small Molecule–Nucleic Acid Interactions, *Methods*, 2007, **42**(2), 150–161, DOI: 10.1016/j.ymeth.2006.09.009.

73 M. Genta, G. Ferrara, R. Capelli, D. Rondelli, S. Sertic, M. Bolognesi, M. Rizzi, F. Rossi, D. Jeruzalmi, A. Chaves-Sanjuan and R. Miggiano, Mechanistic Understanding of UvrA Damage Detection and Lesion Hand-off to UvrB in Nucleotide Excision Repair, *Nat. Commun.*, 2025, **16**(1), 3416, DOI: 10.1038/s41467-025-58670-0.

74 D. Capelli, V. Scognamiglio and R. Montanari, Surface Plasmon Resonance Technology: Recent Advances, Applications and Experimental Cases, *TrAC, Trends Anal. Chem.*, 2023, **163**, 117079, DOI: 10.1016/j.trac.2023.117079.

75 J. Zhang, B. Liu, H. Chen, L. Zhang and X. Jiang, Application and Method of Surface Plasmon Resonance Technology in the Preparation and Characterization of Biomedical Nanoparticle Materials, *Int. J. Nanomed.*, 2024, **19**, 7049–7069, DOI: 10.2147/IJN.S468695.

76 J. Li, P. Yao, K. Tang, X. Zhao, X. Liu, Q. Liu, T. Wei, H. Xuan, S. Bian, Y. Guo, Z. Yang, Z.-Q. Zhang and L. Zhang, Functional Aptamers In Vitro Evolution for Intranuclear Blockage of RNA-Protein Interaction, *J. Am. Chem. Soc.*, 2024, **146**(35), 24654–24662, DOI: 10.1021/jacs.4c08824.

77 R. D. Overacker, B. Plitzko and S. Loesgen, Biolayer Interferometry Provides a Robust Method for Detecting DNA Binding Small Molecules in Microbial Extracts, *Anal. Bioanal. Chem.*, 2021, **413**(4), 1159–1171, DOI: 10.1007/s00216-020-03079-5.

78 C. I. Cheng, Y.-P. Chang and Y.-H. Chu, Biomolecular Interactions and Tools for Their Recognition: Focus on the Quartz Crystal Microbalance and Its Diverse Surface Chemistries and Applications, *Chem. Soc. Rev.*, 2012, **41**(5), 1947–1971, DOI: 10.1039/C1CS15168A.
79 H. Müller-Esparza, M. Osorio-Valeriano, N. Steube, M. Thanbichler and L. Randau, Bio-Layer Interferometry Analysis of the Target Binding Activity of CRISPR-Cas Effector Complexes, *Front. Mol. Biosci.*, 2020, 7, DOI: 10.3389/fmolb.2020.00098.
80 M. Rieu, J. Valle-Orero, B. Ducos, J.-F. Allemand and V. Croquette, Single-Molecule Kinetic Locking Allows Fluorescence-Free Quantification of Protein/Nucleic-Acid Binding, *Commun. Biol.*, 2021, **4**(1), 1083, DOI: 10.1038/s42003-021-02606-z.
81 A. Lostao, K. Lim, M. C. Pallarés, A. Ptak and C. Marcuello, Recent Advances in Sensing the Inter-Biomolecular Interactions at the Nanoscale – A Comprehensive Review of AFM-Based Force Spectroscopy, *Int. J. Biol. Macromol.*, 2023, **238**, 124089, DOI: 10.1016/j.ijbiomac.2023.124089.
82 Š. Ivanovaitė, J. Paksaitė, A. Kopūstas, G. Karzaitė, D. Rutkauskas, A. Silanskas, G. Sasnauskas, M. Zaremba, S. K. Jones Jr. and M. Tutkus, smFRET Detection of Cis and Trans DNA Interactions by the BfiI Restriction Endonuclease, *J. Phys. Chem. B*, 2023, **127**(29), 6470–6478, DOI: 10.1021/acs.jpcb.3c03269.
83 T. Plénat, C. Tardin, P. Rousseau and L. Salomé, High-Throughput Single-Molecule Analysis of DNA–Protein Interactions by Tethered Particle Motion, *Nucleic Acids Res.*, 2012, **40**(12), e89, DOI: 10.1093/nar/gks250.
84 Freely orbiting magnetic tweezers to directly monitor changes in the twist of nucleic acids | Nature Communications. https://www.nature.com/articles/ncomms1450#change-history (accessed 2025-06-14).
85 E. Beckwitt, M. Kong and B. Van Houten, Studying Protein-DNA Interactions Using Atomic Force Microscopy, *Semin. Cell Dev. Biol.*, 2018, **73**, 220–230, DOI: 10.1016/j.semcdb.2017.06.028.
86 K. C. Neuman and A. Nagy, Single-Molecule Force Spectroscopy: Optical Tweezers, Magnetic Tweezers and Atomic Force Microscopy, *Nat. Methods*, 2008, **5**(6), 491–505, DOI: 10.1038/nmeth.1218.
87 D. Y. Zhang and G. Seelig, Dynamic DNA Nanotechnology Using Strand-Displacement Reactions, *Nat. Chem.*, 2011, **3**(2), 103–113, DOI: 10.1038/nchem.957.
88 Y. Guo, B. Wei, S. Xiao, D. Yao, H. Li, H. Xu, T. Song, X. Li and H. Liang, Recent Advances in Molecular Machines Based on Toehold-Mediated Strand Displacement Reaction, *Quant. Biol.*, 2017, **5**(1), 25–41, DOI: 10.1007/s40484-017-0097-2.
89 F. C. Simmel, B. Yurke and H. R. Singh, Principles and Applications of Nucleic Acid Strand Displacement Reactions, *Chem. Rev.*, 2019, **119**(10), 6326–6369, DOI: 10.1021/acs.chemrev.8b00580.
90 M. Xiao, W. Lai, T. Man, B. Chang, L. Li, A. R. Chandrasekaran and H. Pei, Rationally Engineered Nucleic Acid Architectures for Biosensing Applications, *Chem. Rev.*, 2019, **119**(22), 11631–11717, DOI: 10.1021/acs.chemrev.9b00121.
91 W. Tang, W. Zhong, Y. Tan, G. A. Wang, F. Li and Y. Liu, DNA Strand Displacement Reaction: A Powerful Tool for Discriminating Single Nucleotide Variants, *Top. Curr. Chem.*, 2020, **378**(1), 10, DOI: 10.1007/s41061-019-0274-z.
92 K. L. Wong and J. Liu, Factors and Methods to Modulate DNA Hybridization Kinetics, *Biotechnol. J.*, 2021, **16**(11), 2000338, DOI: 10.1002/biot.202000338.
93 T. Tian, Y. Li and Y. Lin, Prospects and Challenges of Dynamic DNA Nanostructures in Biomedical Applications, *Bone Res.*, 2022, **10**(1), 1–15, DOI: 10.1038/s41413-022-00212-1.
94 L. Qian, E. Winfree and J. Bruck, Neural Network Computation with DNA Strand Displacement Cascades, *Nature*, 2011, **475**(7356), 368–372, DOI: 10.1038/nature10262.
95 Y. Liu, Z. Zhao, Y. Zeng, M. He, Y. Lyu and Q. Yuan, Thermodynamics and Kinetics-Directed Regulation of Nucleic Acid-Based Molecular Recognition, *Small Methods*, 2024, 2401102, DOI: 10.1002/smtd.202401102.
96 B. Ashwood and A. Tokmakoff, Kinetics and Dynamics of Oligonucleotide Hybridization, *Nat. Rev. Chem.*, 2025, 1–23, DOI: 10.1038/s41570-025-00704-8.
97 E. Del Grosso, E. Franco, L. J. Prins and F. Ricci, Dissipative DNA Nanotechnology, *Nat. Chem.*, 2022, **14**(6), 600–613, DOI: 10.1038/s41557-022-00957-6.
98 S. M. Douglas, H. Dietz, T. Liedl, B. Högberg, F. Graf and W. M. Shih, Self-Assembly of DNA into Nanoscale Three-Dimensional Shapes, *Nature*, 2009, **459**(7245), 414–418, DOI: 10.1038/nature08016.
99 B. Yurke, A. J. Turberfield, A. P. Mills, F. C. Simmel and J. L. Neumann, A DNA-Fuelled Molecular Machine Made of DNA, *Nature*, 2000, **406**(6796), 605–608, DOI: 10.1038/35020524.
100 D. Y. Zhang and E. Winfree, Control of DNA Strand Displacement Kinetics Using Toehold Exchange, *J. Am. Chem. Soc.*, 2009, **131**(47), 17303–17314, DOI: 10.1021/ja906987s.
101 Z. Guo, Q. Liu and L. M. Smith, Enhanced Discrimination of Single Nucleotide Polymorphisms by Artificial Mismatch Hybridization, *Nat. Biotechnol.*, 1997, **15**(4), 331–335, DOI: 10.1038/nbt0497-331.
102 S. X. Chen, D. Y. Zhang and G. Seelig, Conditionally Fluorescent Molecular Probes for Detecting Single Base Changes in Double-Stranded DNA, *Nat. Chem.*, 2013, **5**(9), 782–789, DOI: 10.1038/nchem.1713.
103 J. S. Wang and D. Y. Zhang, Simulation-Guided DNA Probe Design for Consistently Ultraspecific Hybridization, *Nat. Chem.*, 2015, **7**(7), 545–553, DOI: 10.1038/nchem.2266.
104 P. Song, S. X. Chen, Y. H. Yan, A. Pinto, L. Y. Cheng, P. Dai, A. A. Patel and D. Y. Zhang, Selective Multiplexed Enrichment for the Detection and Quantitation of Low-Fraction DNA Variants via Low-Depth Sequencing, *Nat. Biomed. Eng.*, 2021, **5**(7), 690–701, DOI: 10.1038/s41551-021-00713-0.
105 J. SantaLucia, A Unified View of Polymer, Dumbbell, and Oligonucleotide DNA Nearest-Neighbor Thermodynamics,

Proc. Natl. Acad. Sci. U. S. A., 1998, **95**(4), 1460–1465, DOI: 10.1073/pnas.95.4.1460.

106 J. SantaLucia and D. Hicks, The Thermodynamics of DNA Structural Motifs, *Annu. Rev. Biophys. Biomol. Struct.*, 2004, **33**(1), 415–440, DOI: 10.1146/annurev.biophys.32.110601.141800.

107 J. H. Bae, J. Z. Fang and D. Y. Zhang, High-Throughput Methods for Measuring DNA Thermodynamics, *Nucleic Acids Res.*, 2020, **48**(15), e89, DOI: 10.1093/nar/gkaa521.

108 G. A. Wang, J. Xu, S. M. Traynor, H. Chen, F. Eljabu, X. Wu, H. Yan and F. Li, DNA Balance for Native Characterization of Chemically Modified DNA, *J. Am. Chem. Soc.*, 2021, **143**(34), 13655–13663, DOI: 10.1021/jacs.1c05236.

109 Y. Wu, G. A. Wang, Q. Yang and F. Li, Native Characterization of Noncanonical Nucleic Acid Thermodynamics via Programmable Dynamic DNA Chemistry, *J. Am. Chem. Soc.*, 2024, **146**(26), 18041–18049, DOI: 10.1021/jacs.4c04721.

110 Y. Wu, Q. Yang, G. A. Wang and F. Li, Native Measurement of Aptamer Folding and Binding Energies Using a Free Energy Shift Assay, *JACS Au*, 2025, **5**(7), 3632–3638, DOI: 10.1021/jacsau.5c00689.

111 J. Xu, G. A. Wang, L. Gao, L. Wu, Q. Lei, H. Deng and F. Li, Enabling Programmable Dynamic DNA Chemistry Using Small-Molecule DNA Binders, *Nat. Commun.*, 2023, **14**(1), 4248, DOI: 10.1038/s41467-023-40032-3.

112 J. Xu, H. Deng, L. Wu, J. Song, X. Feng, Y. Liu, G. A. Wang and F. Li, Binder-Responsive DNA Strand Displacement Enables High-Throughput and High-Fidelity Discovering of Small Molecular DNA Binders, *Anal. Chem.*, 2024, **96**(30), 12213–12216, DOI: 10.1021/acs.analchem.4c02520.

113 J. SantaLucia, How Much Free Energy Is Absorbed upon Breaking DNA Base Pairs?, Comment on ''DNA Melting and Energetics of the Double Helix'' by Maxim Frank-Kamenetskii et Al, *Phys. Life Rev.*, 2018, **25**, 29–33, DOI: 10.1016/j.plrev.2018.03.008.

114 M. Lane, The Thermodynamic Advantage of DNA Oligonucleotide ''stacking Hybridization'' Reactions: Energetics of a DNA Nick, *Nucleic Acids Res.*, 1997, **25**(3), 611–617, DOI: 10.1093/nar/25.3.611.

115 E. Protozanova, P. Yakovchuk and M. D. Frank-Kamenetskii, Stacked–Unstacked Equilibrium at the Nick Site of DNA, *J. Mol. Biol.*, 2004, **342**(3), 775–785, DOI: 10.1016/j.jmb.2004.07.075.

116 A. Vologodskii and M. D. Frank-Kamenetskii, DNA Melting and Energetics of the Double Helix, *Phys. Life Rev.*, 2018, **25**, 1–21, DOI: 10.1016/j.plrev.2017.11.012.

117 P. Yakovchuk, E. Protozanova and M. D. Frank-Kamenetskii, Base-Stacking and Base-Pairing Contributions into Thermal Stability of the DNA Double Helix, *Nucleic Acids Res.*, 2006, **34**(2), 564–574, DOI: 10.1093/nar/gkj454.

118 A. Idili, F. Ricci and A. Vallée-Bélisle, Determining the Folding and Binding Free Energy of DNA-Based Nanodevices and Nanoswitches Using Urea Titration Curves, *Nucleic Acids Res.*, 2017, **45**(13), 7571–7580, DOI: 10.1093/nar/gkx498.

119 H. Qu, Q. Ma, L. Wang, Y. Mao, M. Eisenstein, H. T. Soh and L. Zheng, Measuring Aptamer Folding Energy Using a Molecular Clamp, *J. Am. Chem. Soc.*, 2020, **142**(27), 11743–11749, DOI: 10.1021/jacs.0c01570.

120 M. Chung, K. Zhou, J. T. Powell, C. Lin and M. A. Schwartz, DNA-Based Molecular Clamp for Probing Protein Interactions and Structure under Force, *ACS Nano*, 2024, **18**(40), 27590–27596, DOI: 10.1021/acsnano.4c08663.

121 Y. Du, C. Ma, Y. Zeng, Y. Liu, Z. Zhao and Y. Lyu, Reducing Measurement Deviation by Metastable DNA Probes for Aptamer Thermodynamic Characterization, *Anal. Chem.*, 2025, **97**(3), 1870–1878, DOI: 10.1021/acs.analchem.4c05900.

122 F. Kilchherr, C. Wachauf, B. Pelz, M. Rief, M. Zacharias and H. Dietz, Single-Molecule Dissection of Stacking Forces in DNA, *Science*, 2016, **353**(6304), aaf5508, DOI: 10.1126/science.aaf5508.

123 J. Schnitzbauer, M. T. Strauss, T. Schlichthaerle, F. Schueder and R. Jungmann, Super-Resolution Microscopy with DNA-PAINT, *Nat. Protoc.*, 2017, **12**(6), 1198–1228, DOI: 10.1038/nprot.2017.024.

124 A. Banerjee, M. Anand, S. Kalita and M. Ganji, Single-Molecule Analysis of DNA Base-Stacking Energetics Using Patterned DNA Nanostructures, *Nat. Nanotechnol.*, 2023, **18**(12), 1474–1482, DOI: 10.1038/s41565-023-01485-1.

125 S. Zhang, J. Li and S.-J. Chen, Machine Learning in RNA Structure Prediction: Advances and Challenges, *Biophys. J.*, 2024, **123**(17), 2647–2657, DOI: 10.1016/j.bpj.2024.01.026.

126 T. Shen, Z. Hu, S. Sun, D. Liu, F. Wong, J. Wang, J. Chen, Y. Wang, L. Hong, J. Xiao, L. Zheng, T. Krishnamoorthi, I. King, S. Wang, P. Yin, J. J. Collins and Y. Li, Accurate RNA 3D Structure Prediction Using a Language Model-Based Deep Learning Approach, *Nat. Methods*, 2024, **21**(12), 2287–2298, DOI: 10.1038/s41592-024-02487-0.

127 H. Hwang, H. Jeon, N. Yeo and D. Baek, Big Data and Deep Learning for RNA Biology, *Exp. Mol. Med.*, 2024, **56**(6), 1293–1321, DOI: 10.1038/s12276-024-01243-w.

